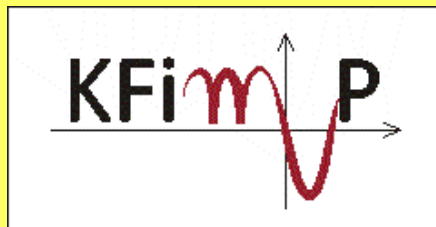


OXIDATION RESISTANT HIGH TEMPERATURE COATINGS

Zbigniew Grzesik

<http://home.agh.edu.pl/~grzesik>

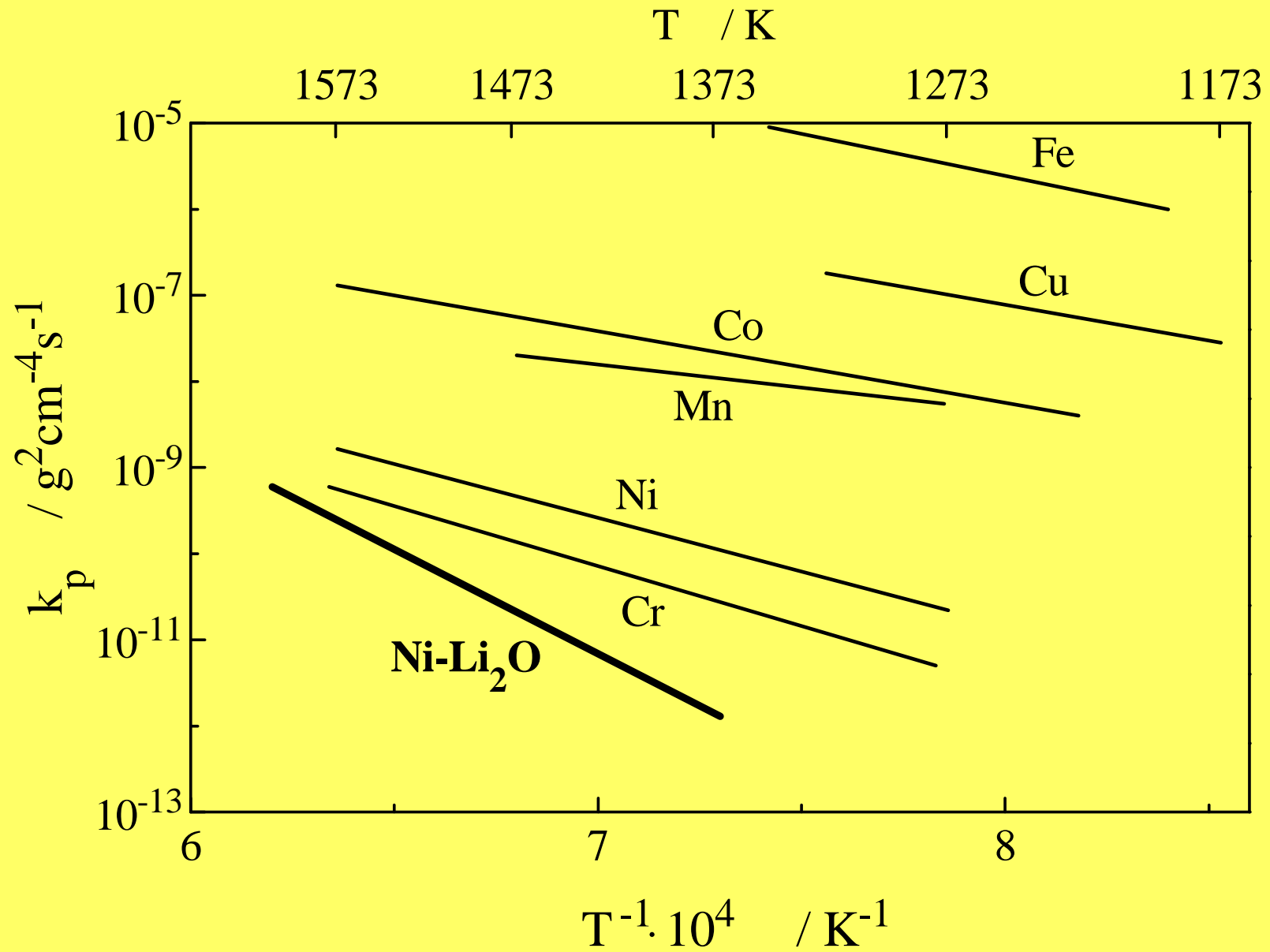


Department of Physical Chemistry and Modelling

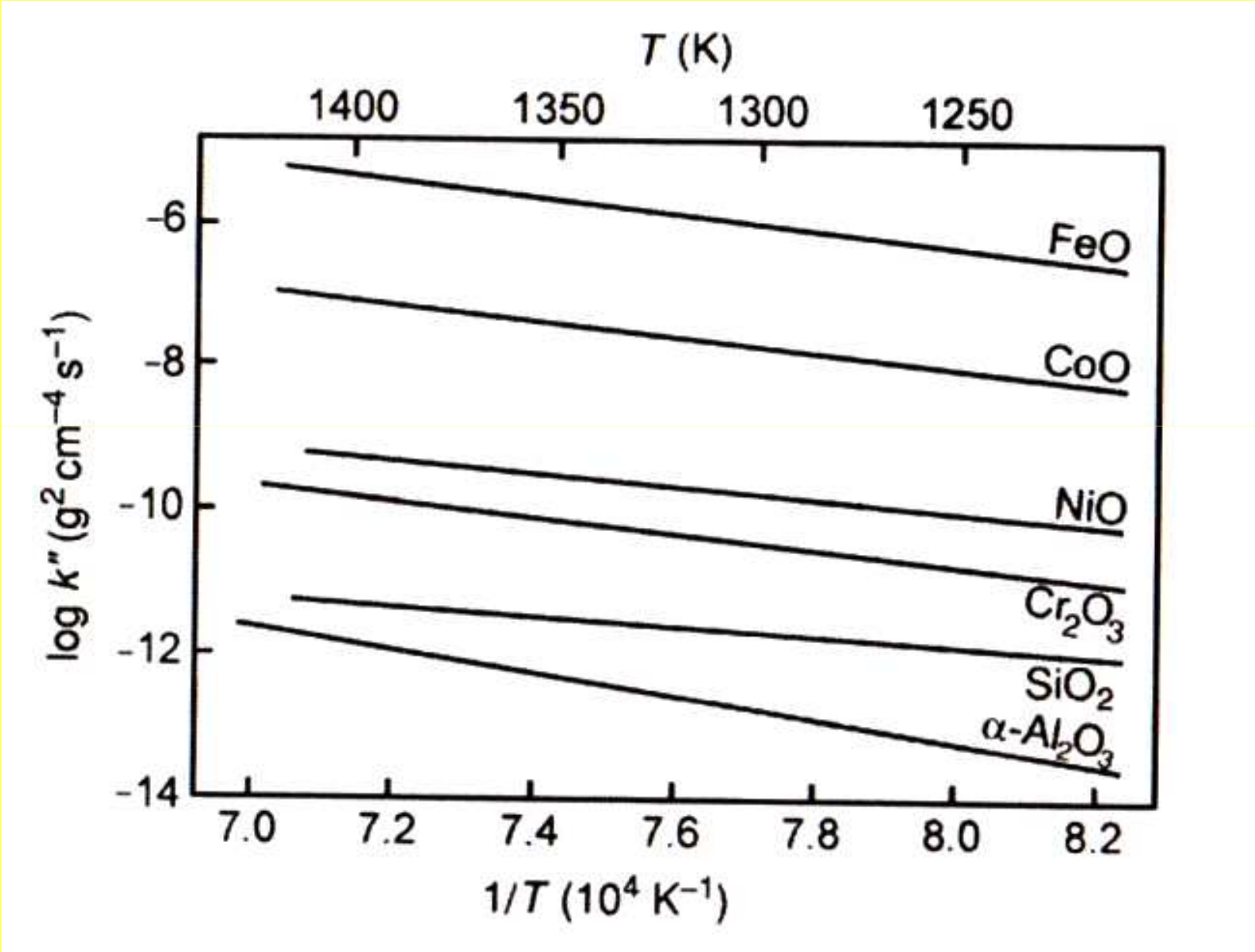
REFERENCES

1. N. Birks, G.H. Meier and F.S Pettit, Introduction to the high temperature oxidation of metals, Cambridge, University Press, 2009.
2. P. Kofstad, „High-Temperature Oxidation of Metals”, John Wiley & Sons, Inc, New York-London-Sydney, 1978.
3. A.S. Khanna, „Introduction to High Temperature Oxidation and Corrosion”, ASM International, Materials Park, 2002.
4. S. Mrowec, „An Introduction to the Theory of Metal Oxidation”, National Bureau of Standards and the National Science Foundation, Washington, D.C., 1982.
5. Wei Gao and Zhengwei Li ”Developments in high-temperature corrosion and protection of metals”, Ed, Woodhead Publishing Limited, Cambridge, England, 2008.
6. R. Cottis, M. Graham, R. Lindsay, S. Lyon, J. Richardson, J. Scantlebury, F. Stott, „Basic Concepts, High Temperature Corrosion”, vol. I, in „Shreir’s Corrosion”, Elsevier, Amsterdam, 2010.

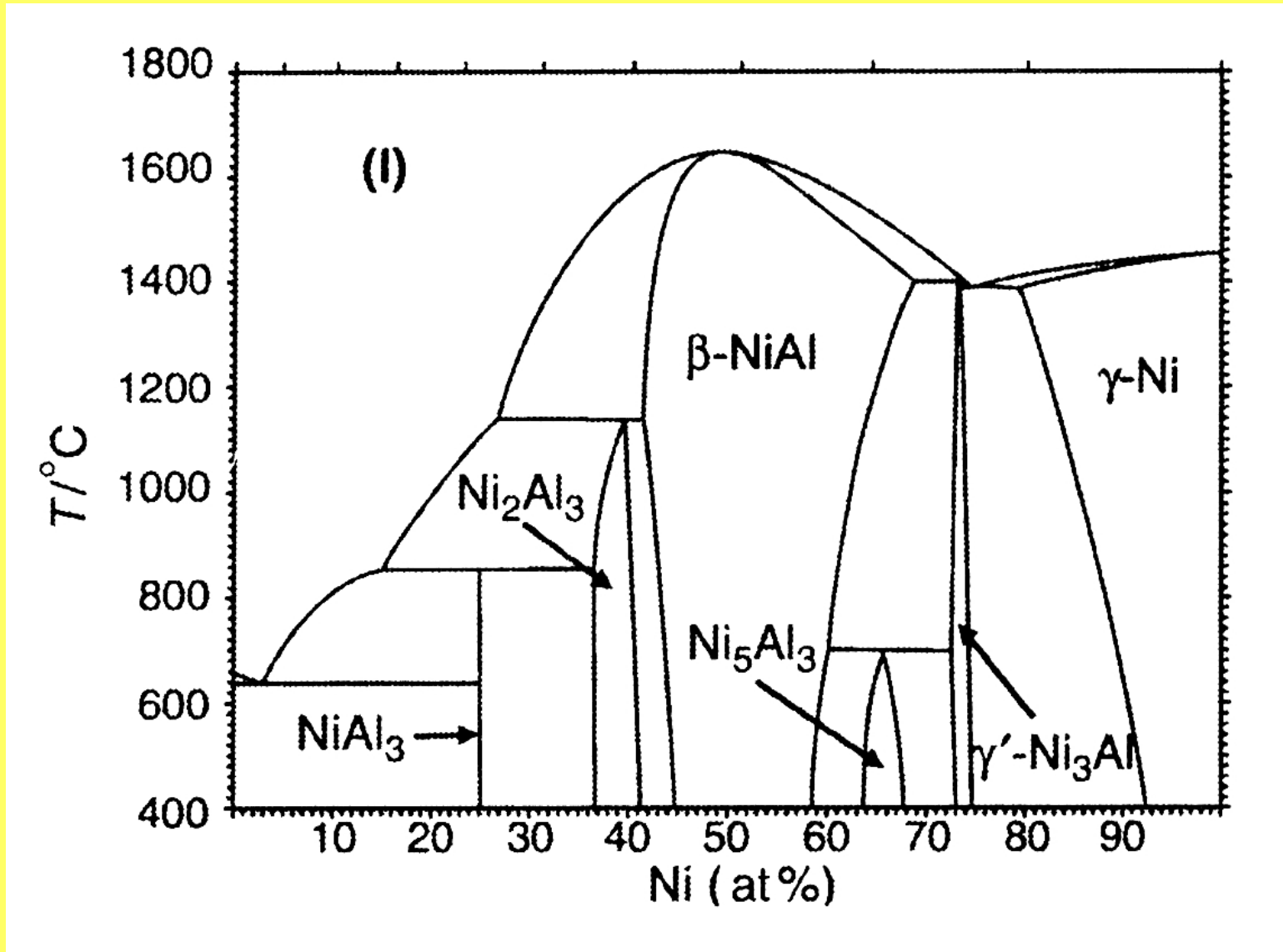
Oxidation resistance of selected metals



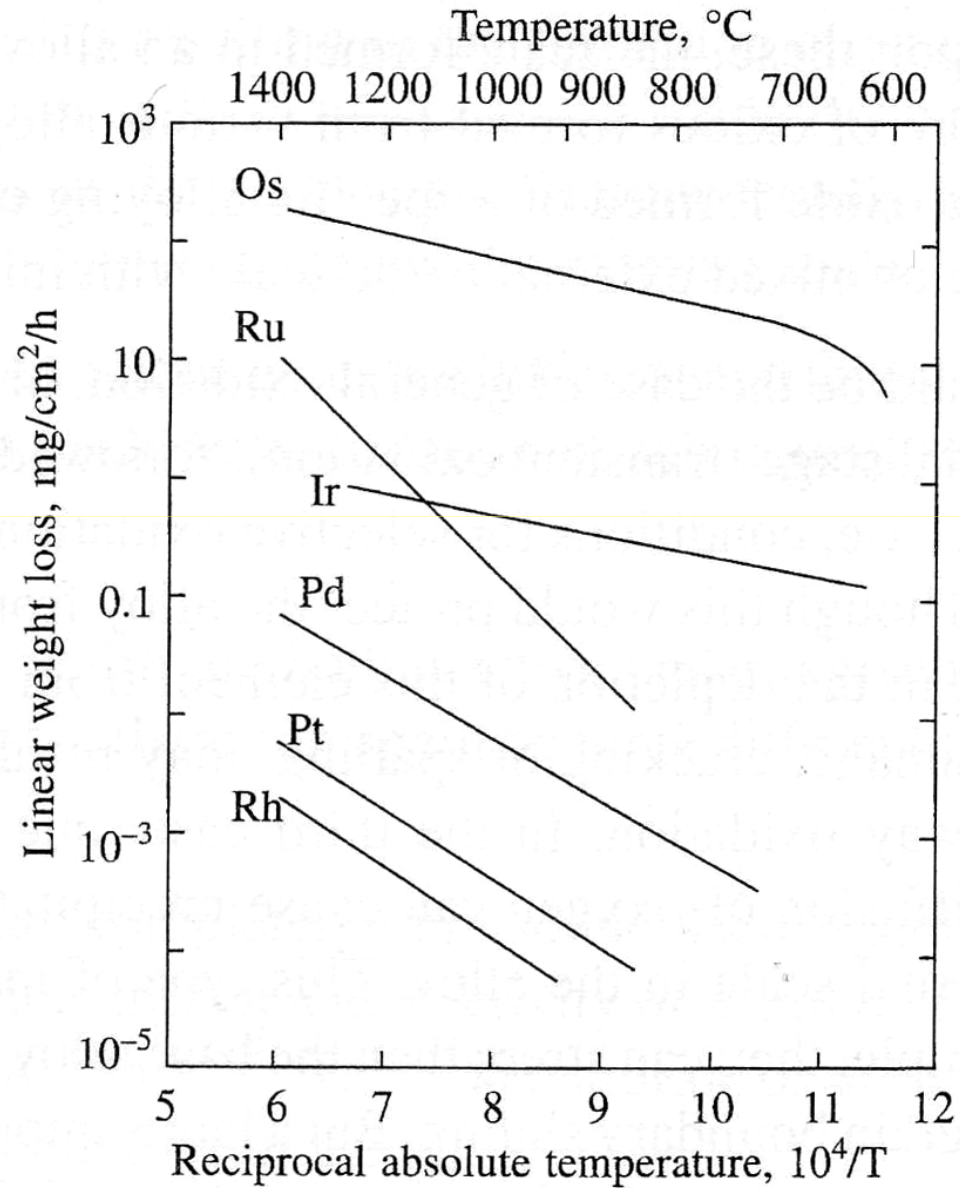
Oxidation resistance of selected metals



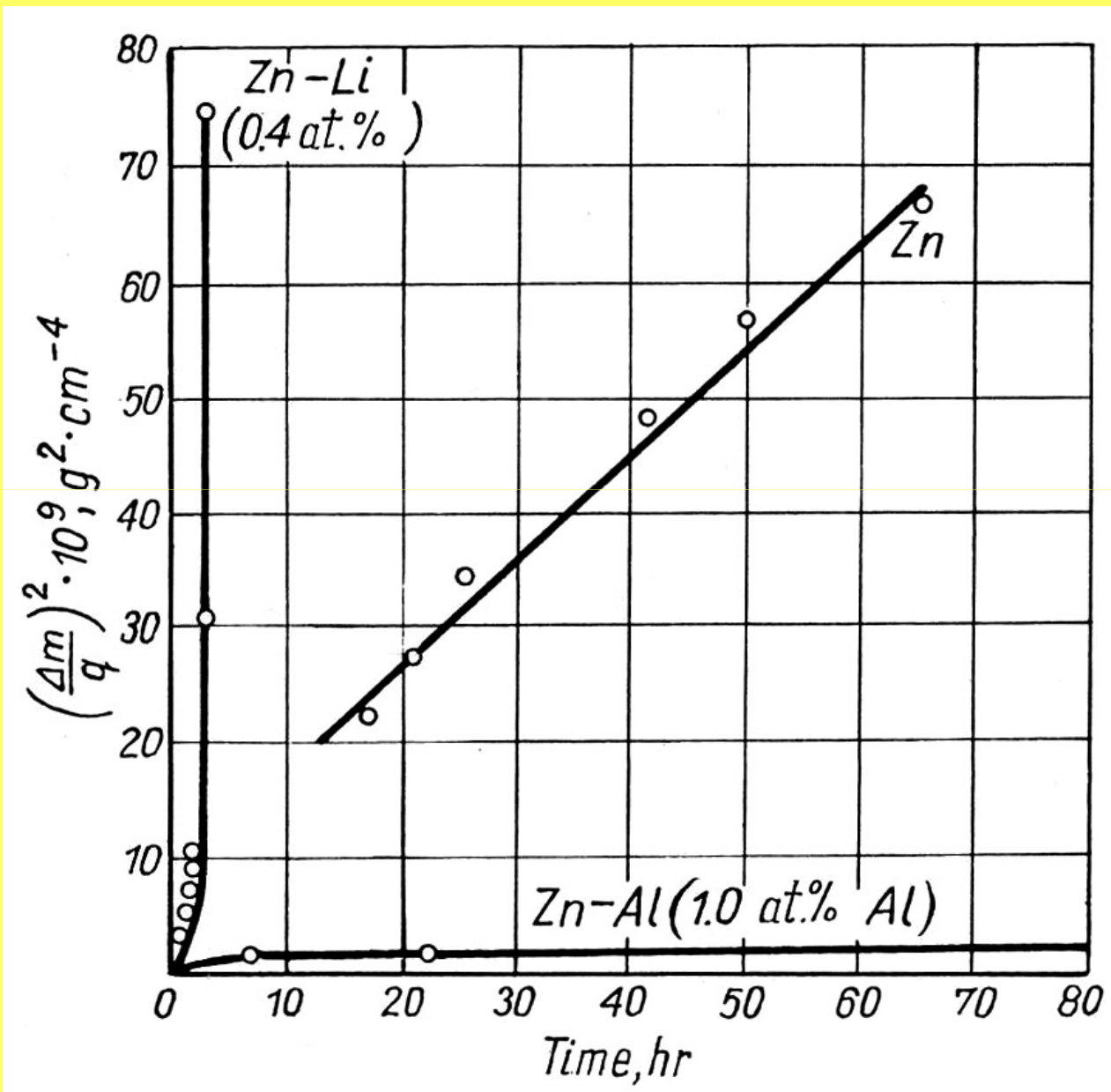
Ni-Al phase diagram



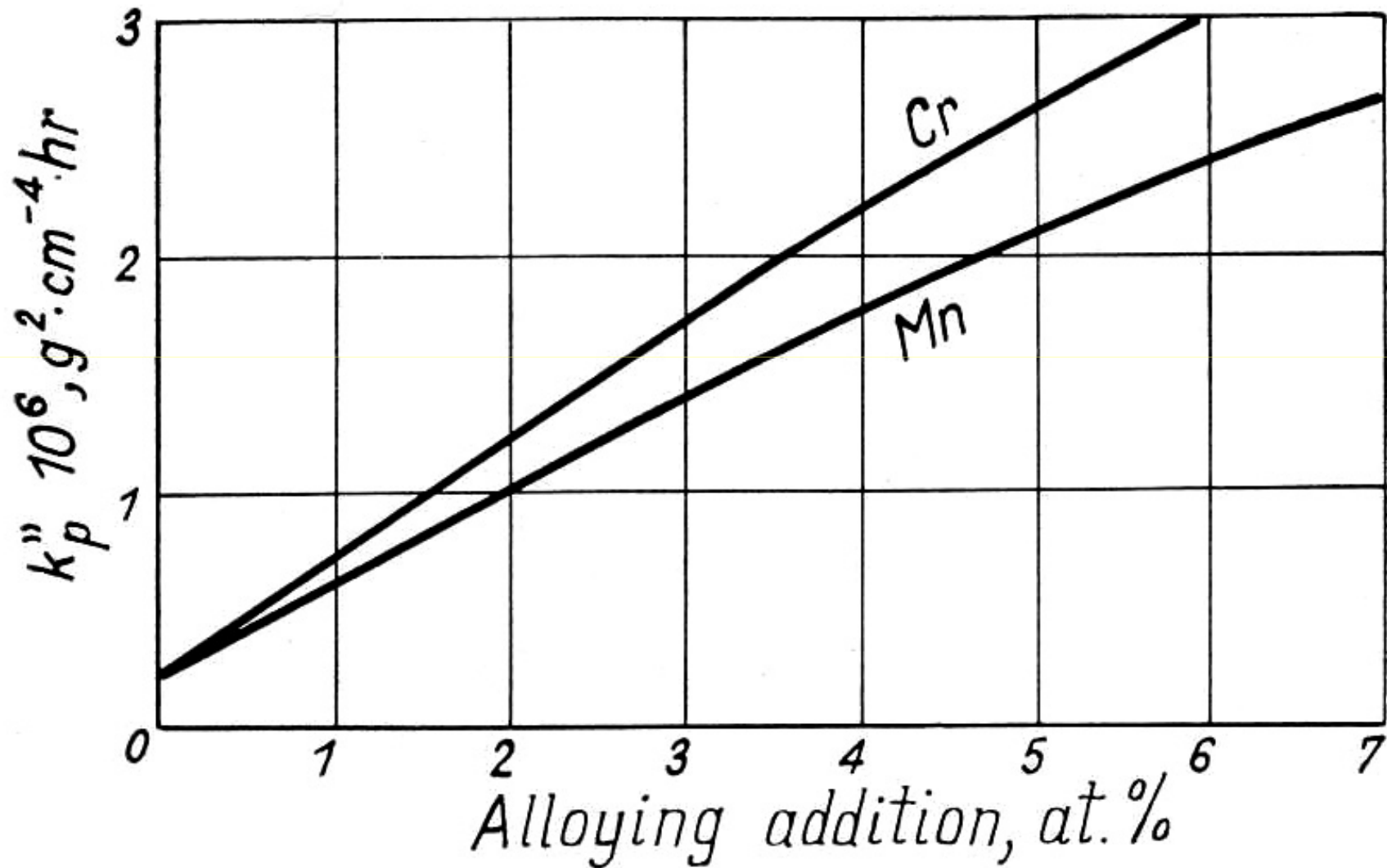
Degradation rate of noble metals at high temperatures



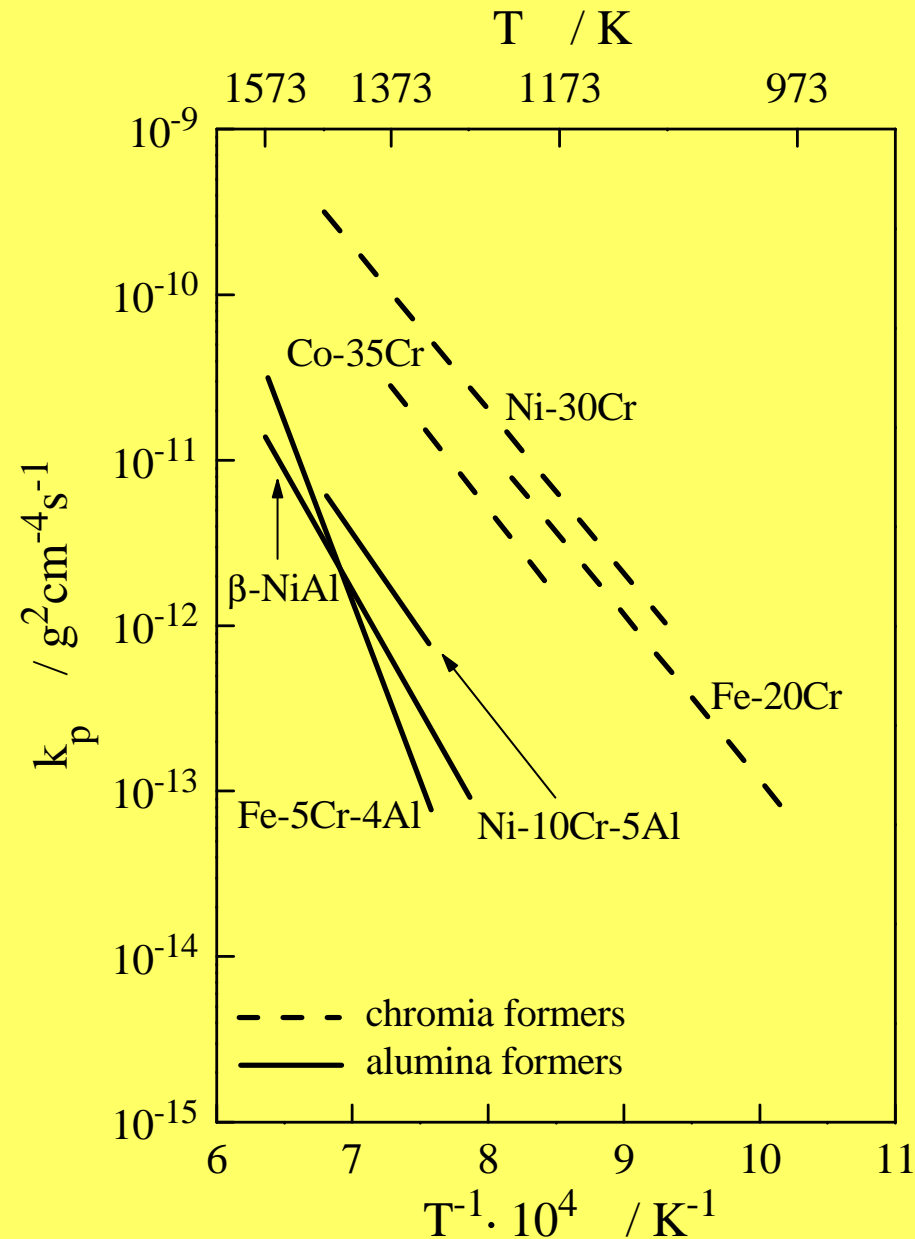
The influence of doping effect on oxidation resistance



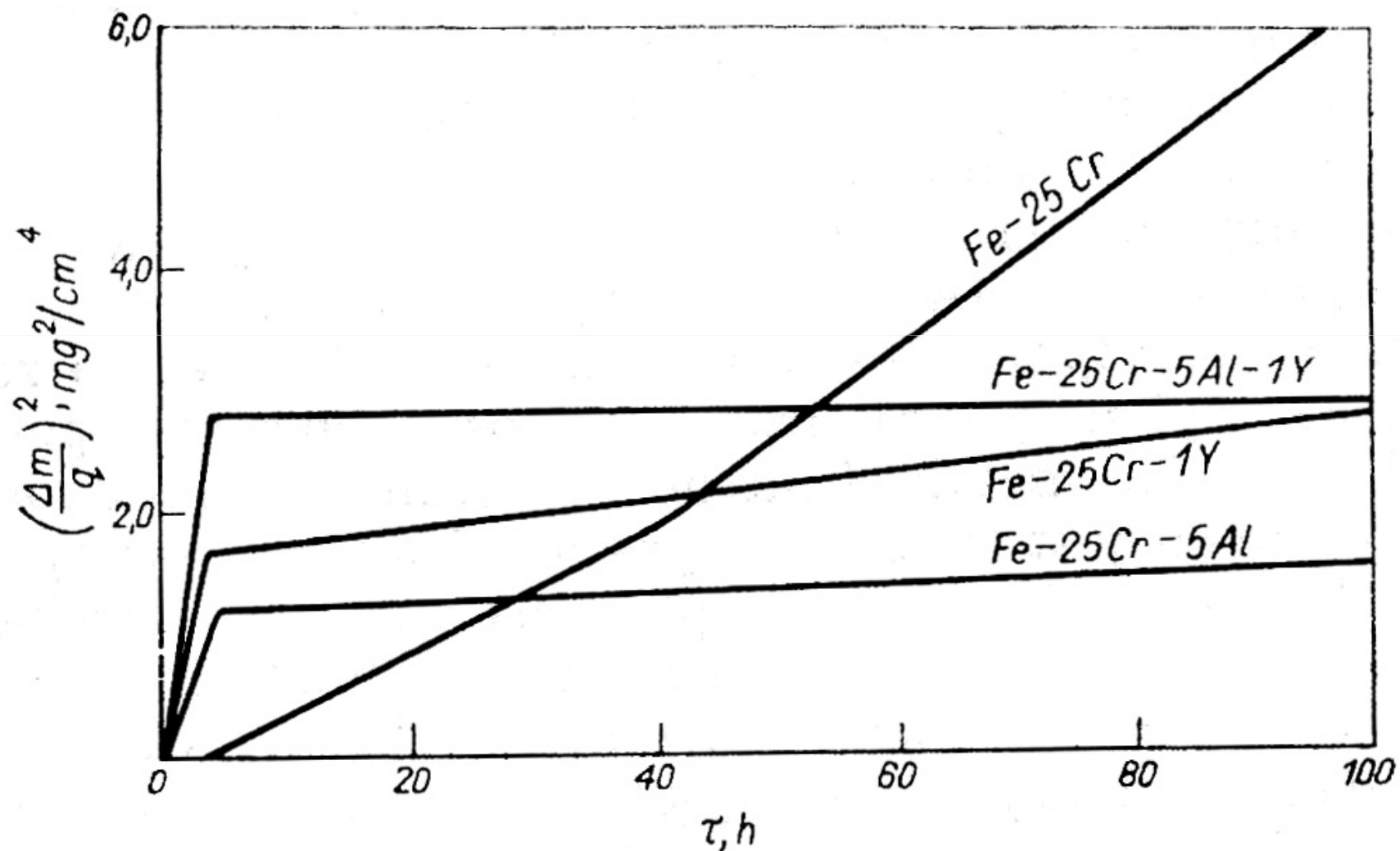
The influence of doping effect on oxidation resistance



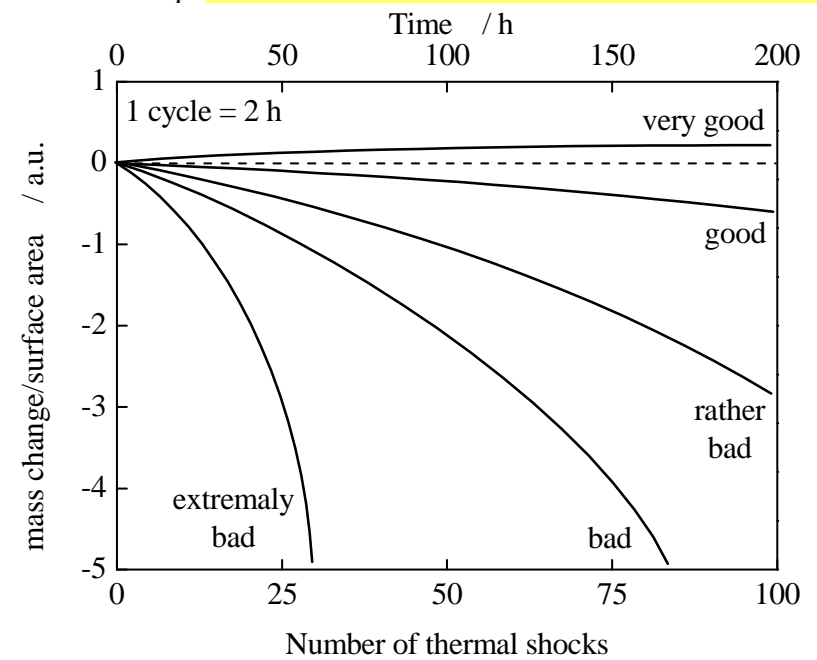
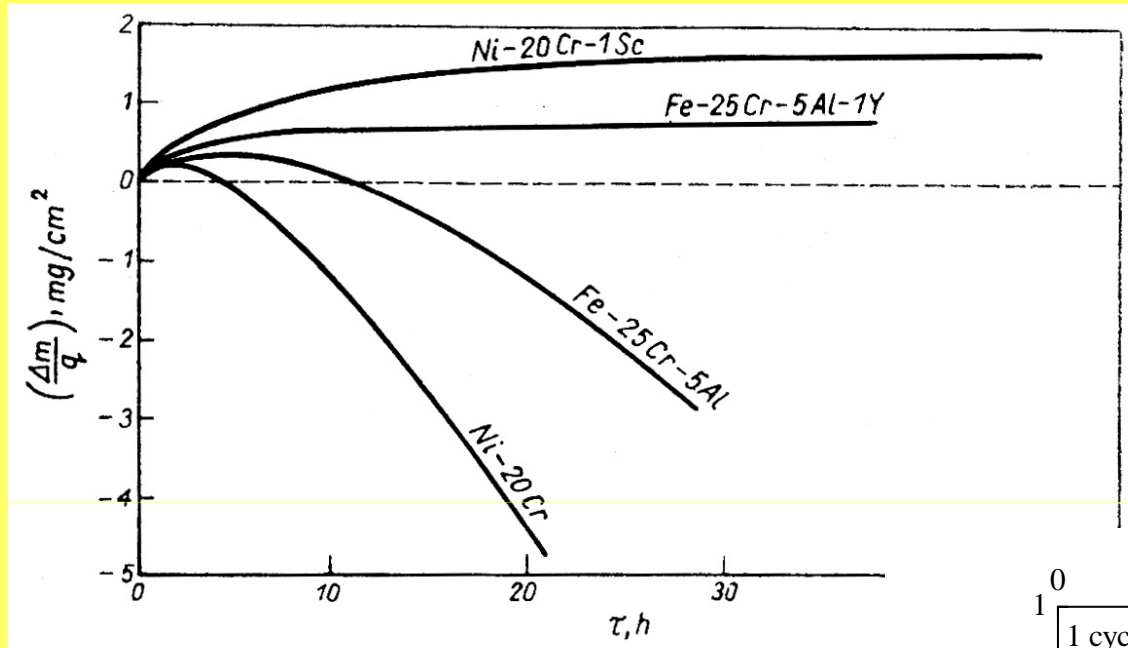
Oxidation resistance of selected alloys



The influence of Y on the oxidation rate of the Fe-25Cr-5Al alloy



The influence of Y and Sc on the degradation rate of the Fe-25Cr-5Al and Ni-20Cr alloys under thermal shock conditions



MATERIALS USED AS PROTECTIVE COATINGS IN OXIDIZING ATMOSPHERES

Cr – Cr₂O₃

Al – Al₂O₃

Si – SiO₂

MCrAlY (where M = Co, Ni, Co/Ni) – Al₂O₃, Cr₂O₃

MCrAlY-Si – Al₂O₃, Cr₂O₃

MCrAlY-RE (where RE = Y, Hf, Zr) – Al₂O₃

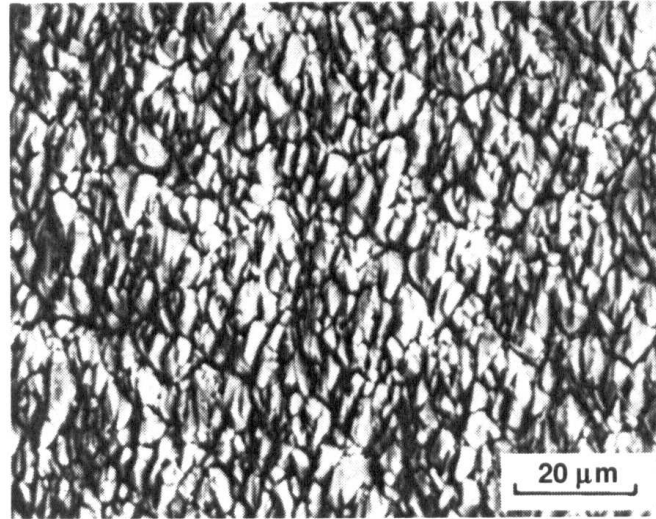
NiAl – Al₂O₃

Cross-section of the Ni-Cr-Al-Y coating obtained by the EB-PVD method

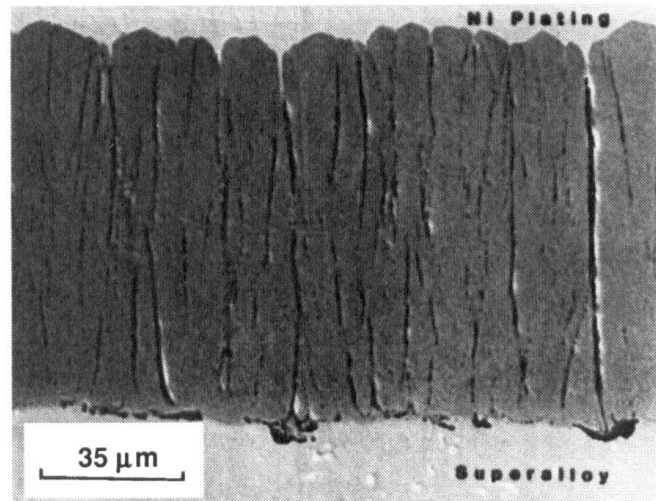


Surface and cross-section of the Co-Cr-Al-Y coating obtained by the EB-PVD method on the IN-738 alloy

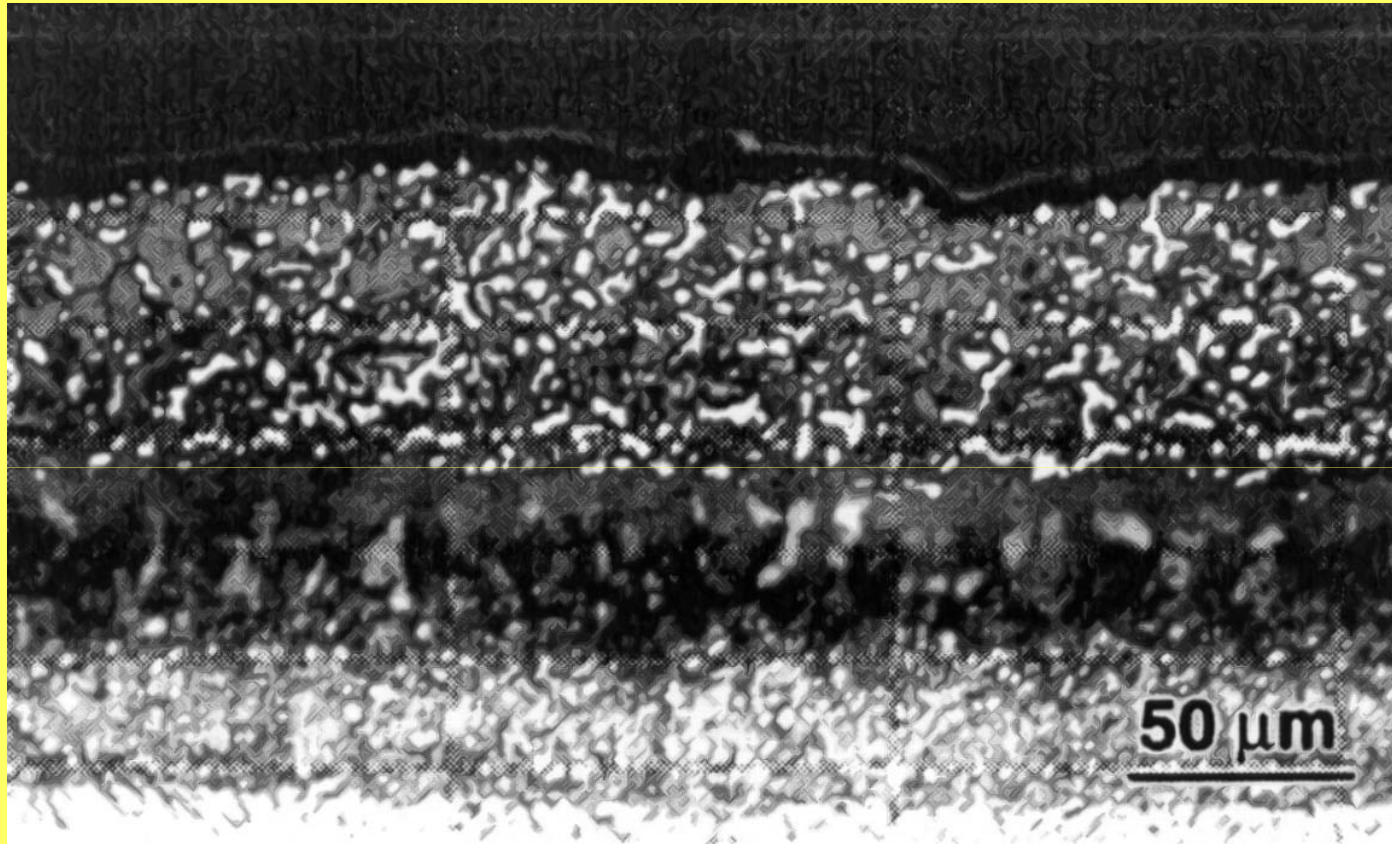
(a)



(b)

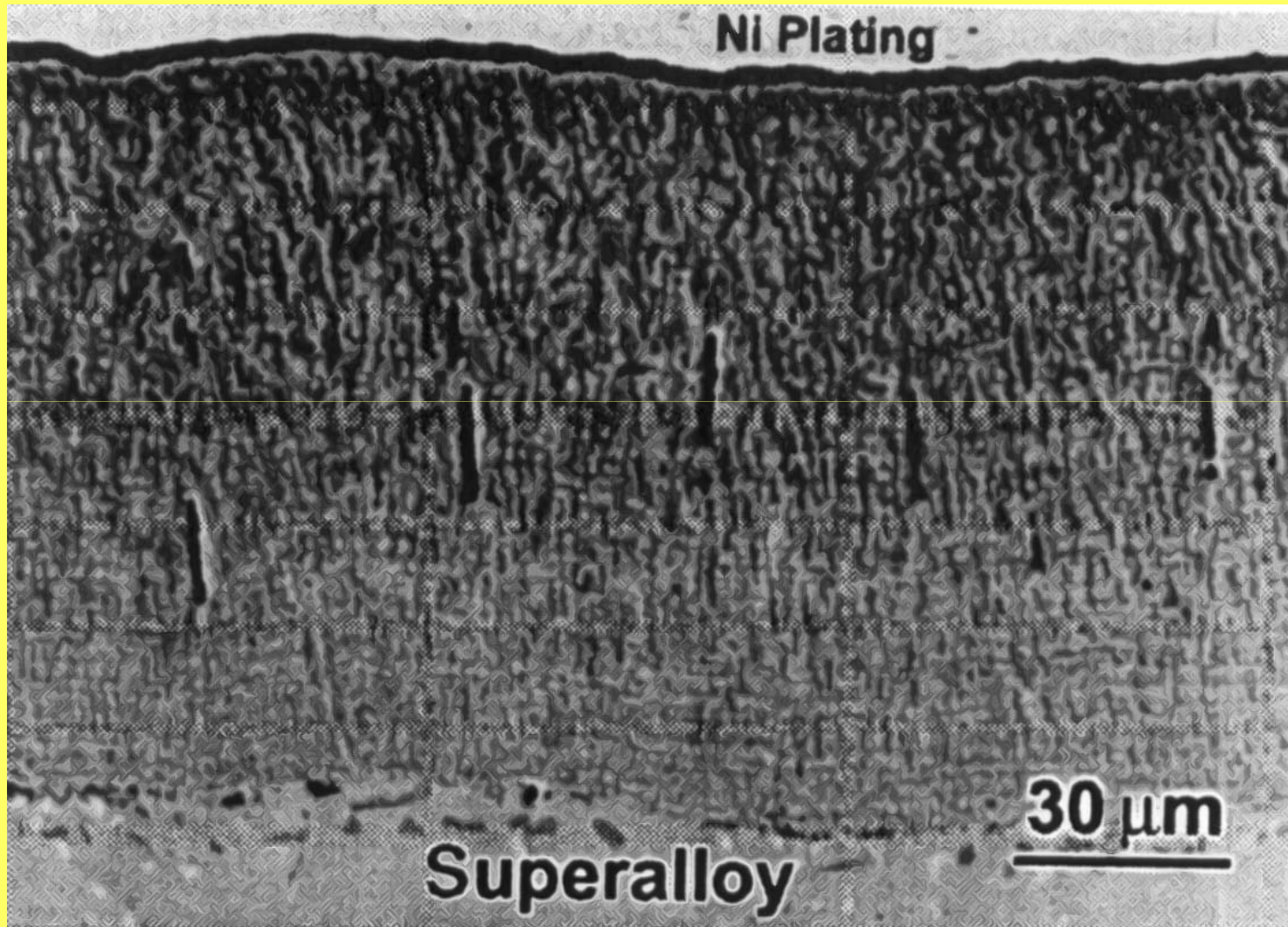


Micrograph of Pt modified aluminide coating on nickel-base superalloy

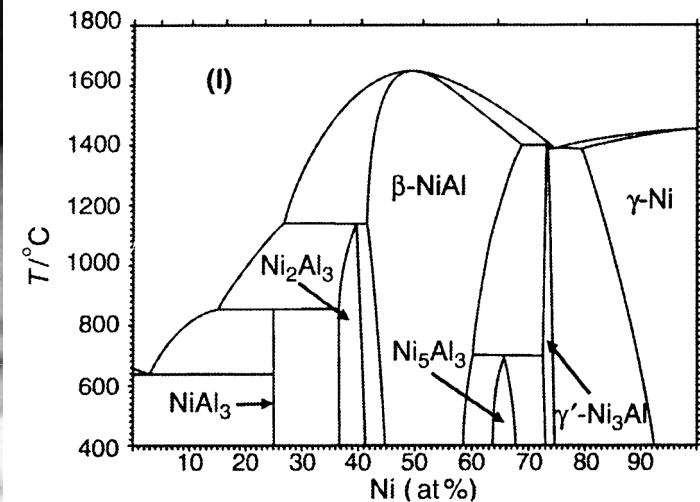
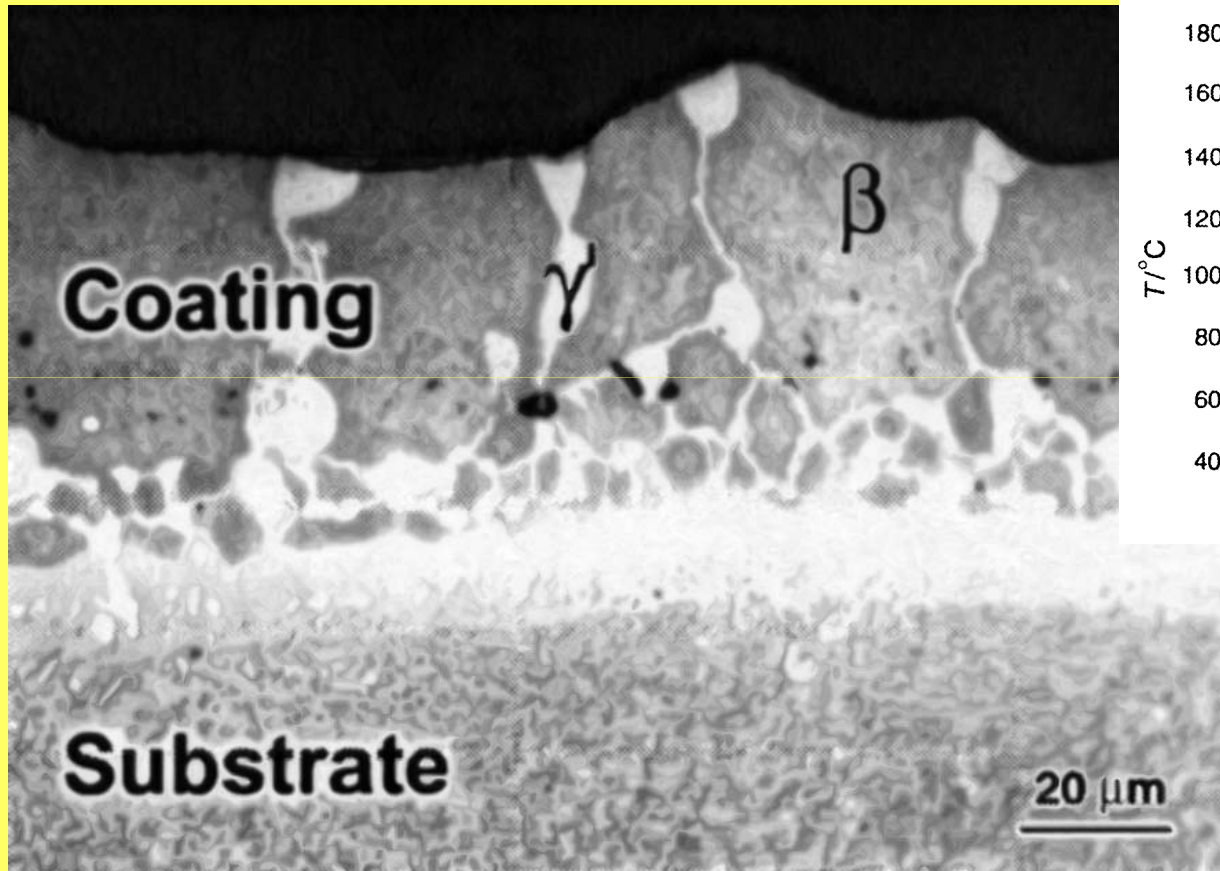


PtAl₂ phase (white color) in a matrix of β-NiAl

Micrograph of cross-section of an EB-PVD
Co-Cr-Al-Y coating, deposited on IN-738

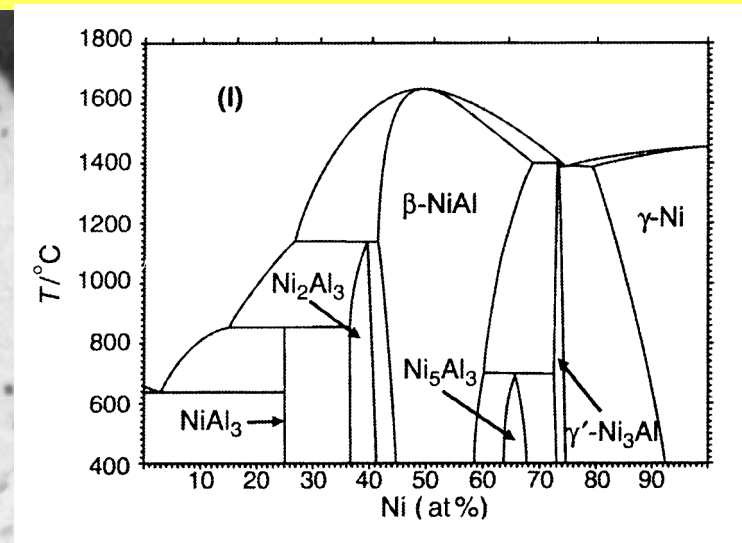
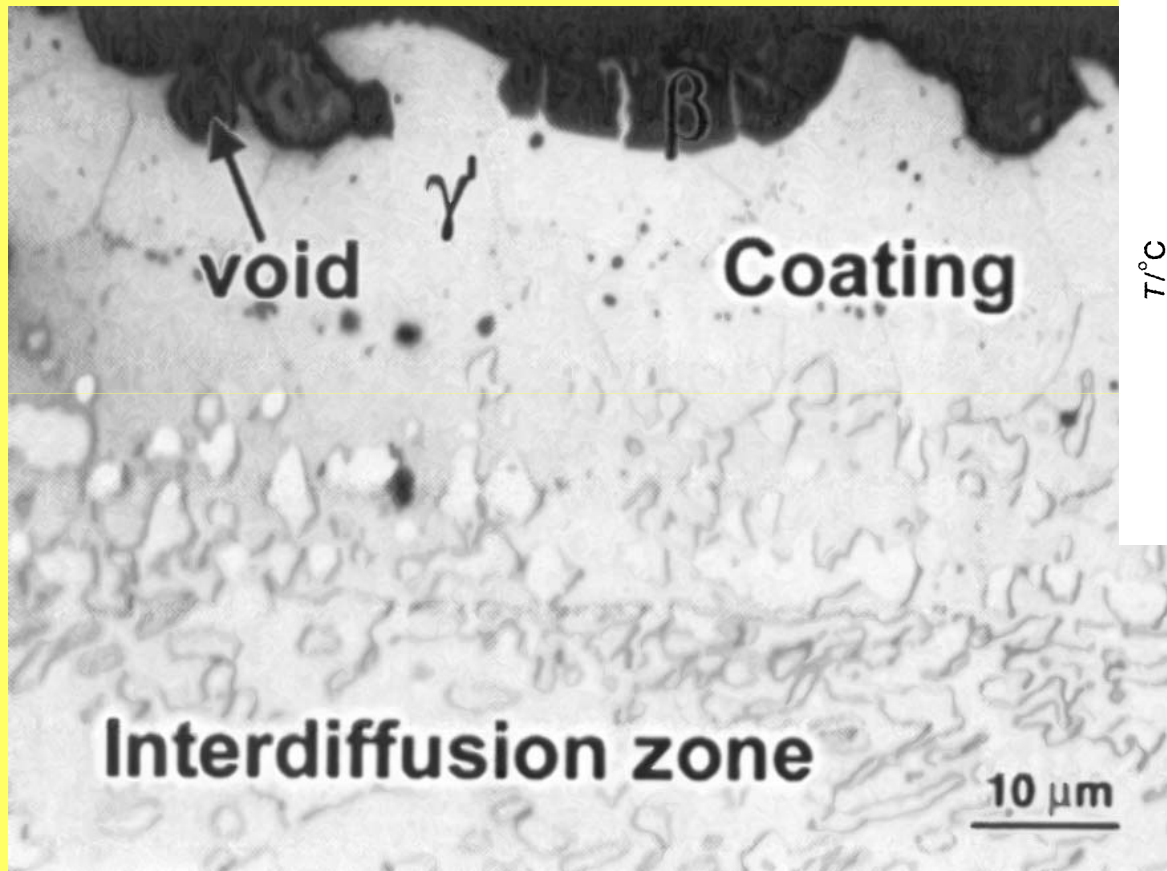


Micrograph of cross-section of Pt-modified aluminide coating on nickel-base single-crystal superalloy after oxidation at 1200°C for 20 h



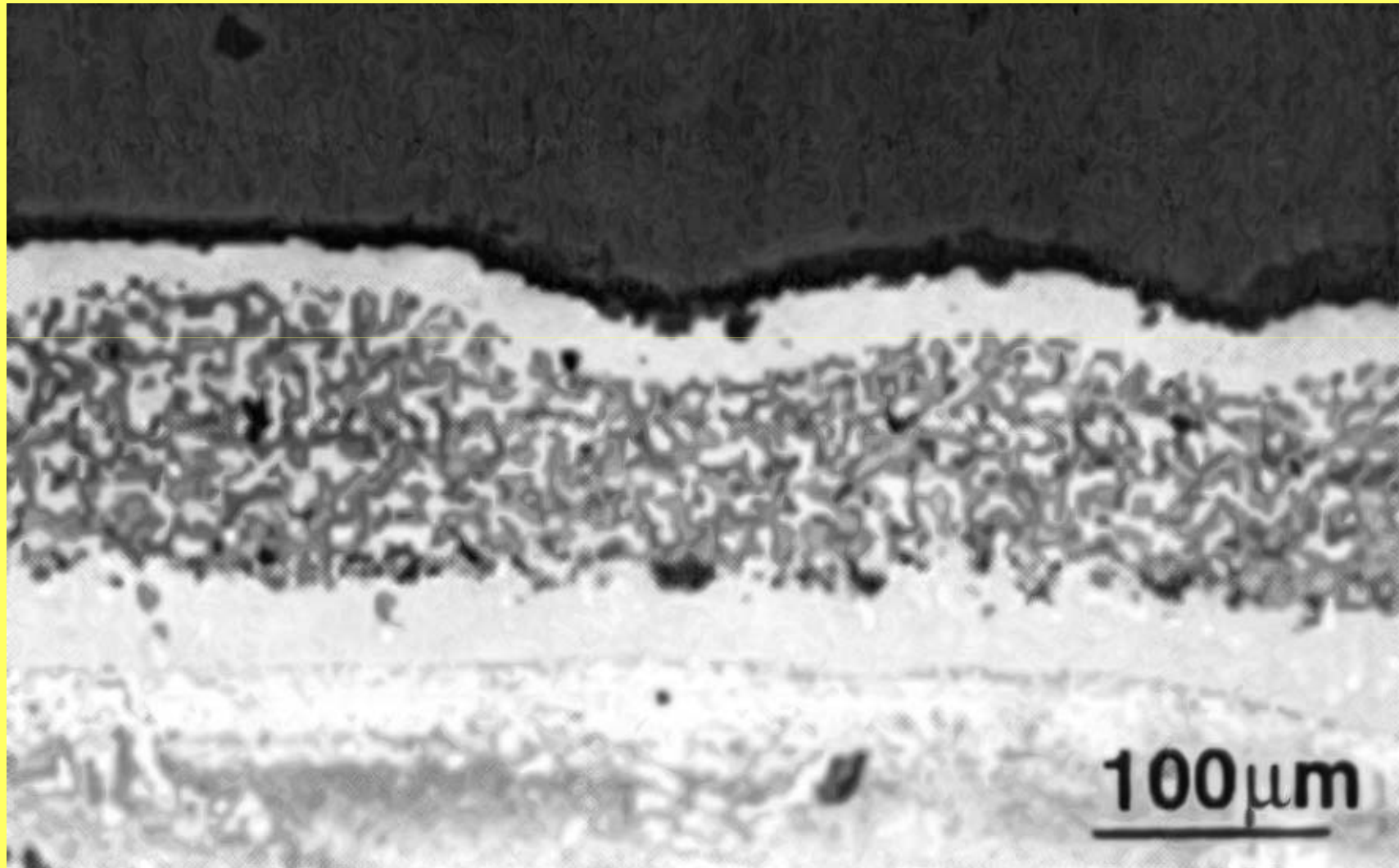
The original grain structure of the β -phase is evident and γ' has begun to nucleate at β grain boundaries as a consequence of Al depletion

Micrograph of cross-section of Pt-modified
aluminide coating on nickel-base single-crystal superalloy
after oxidation at 1200°C for 200 h

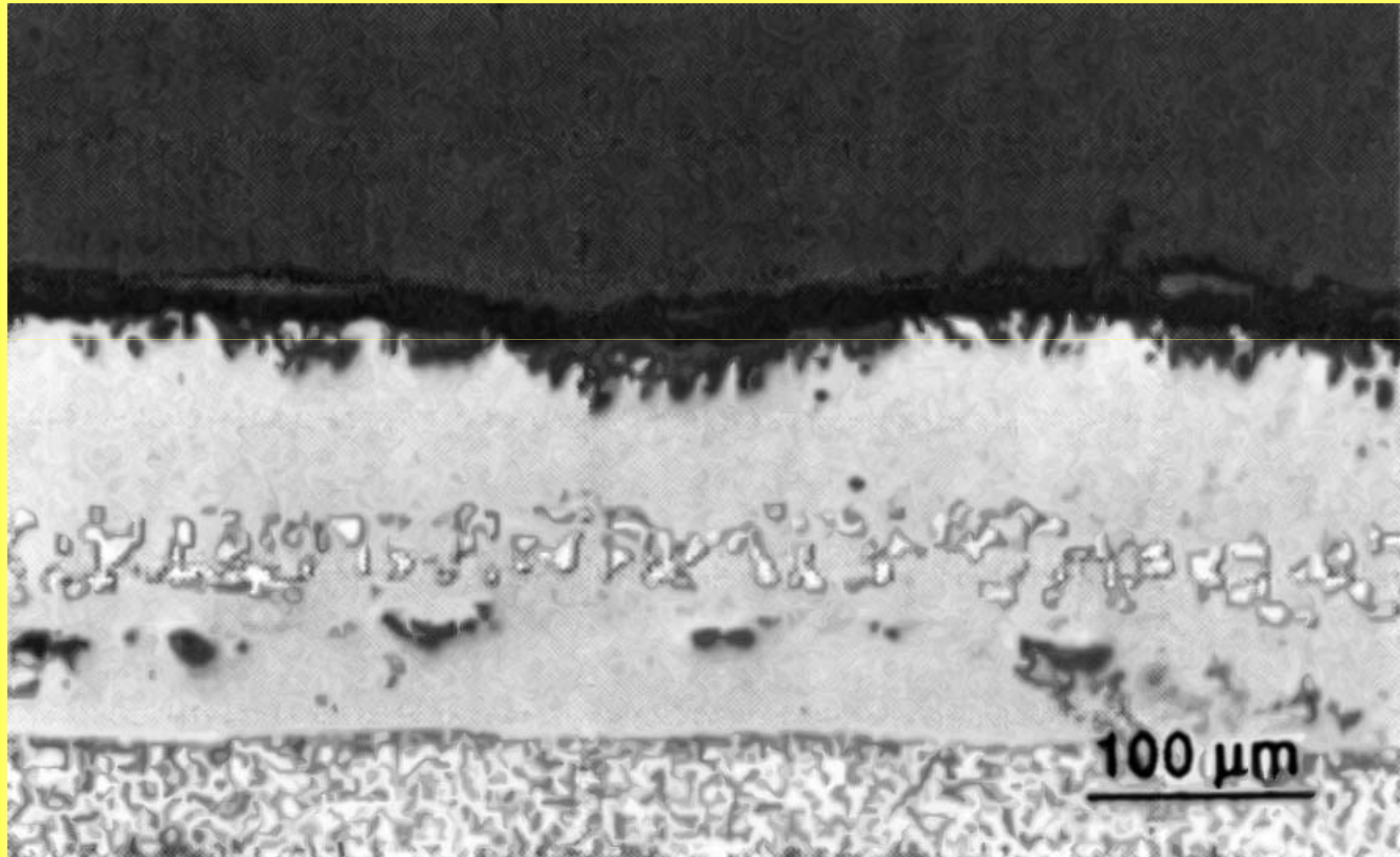


The coating had been converted almost completely to γ' , as a result of Al depletion. Further exposure would result in the γ' transforming to γ .

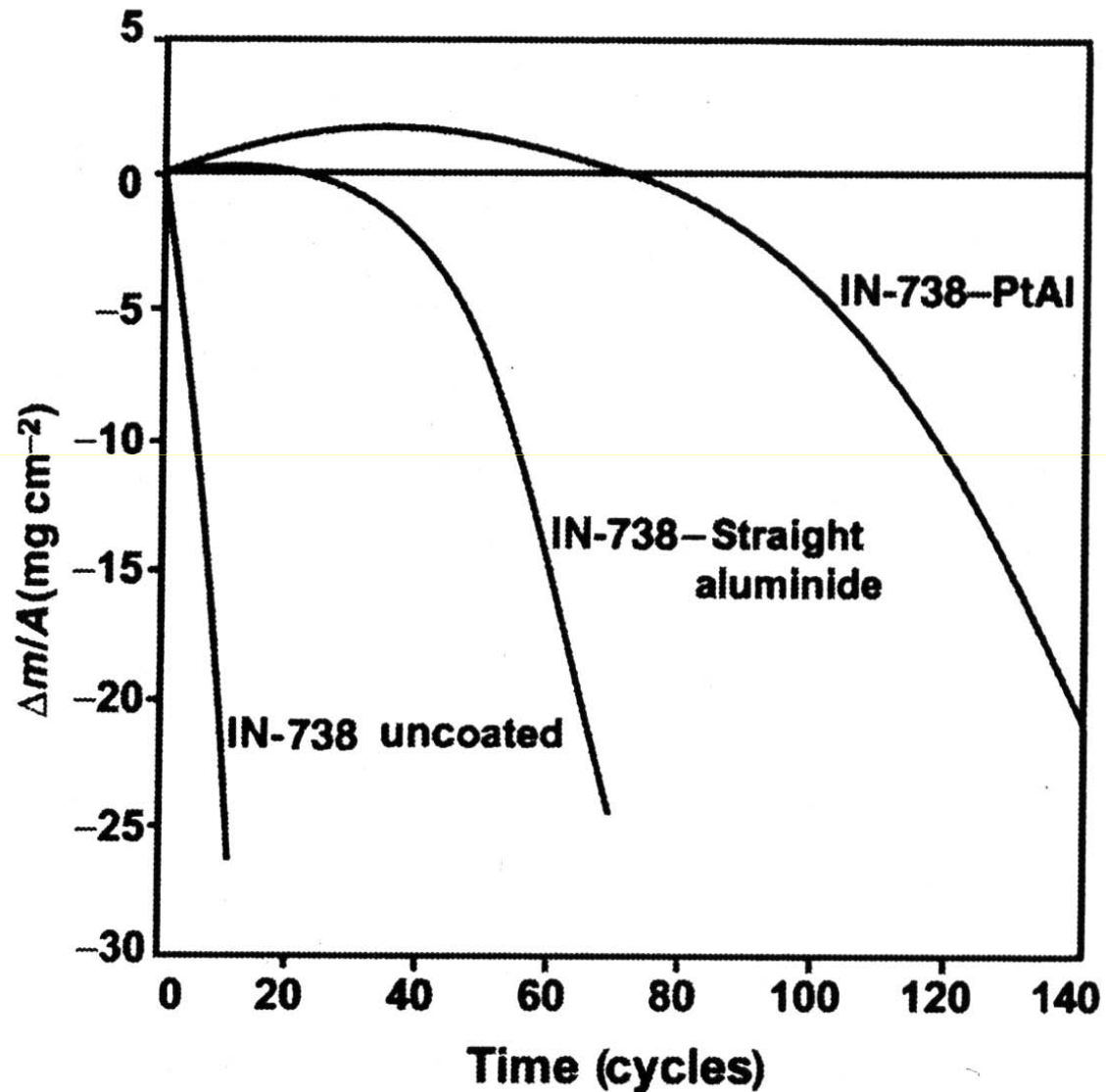
Micrograph of cross-section of a Ni-Co-Cr-Al-Y coating on a single-crystal Ni-base superalloy after 200 one-hour cycles at 1100°C in air



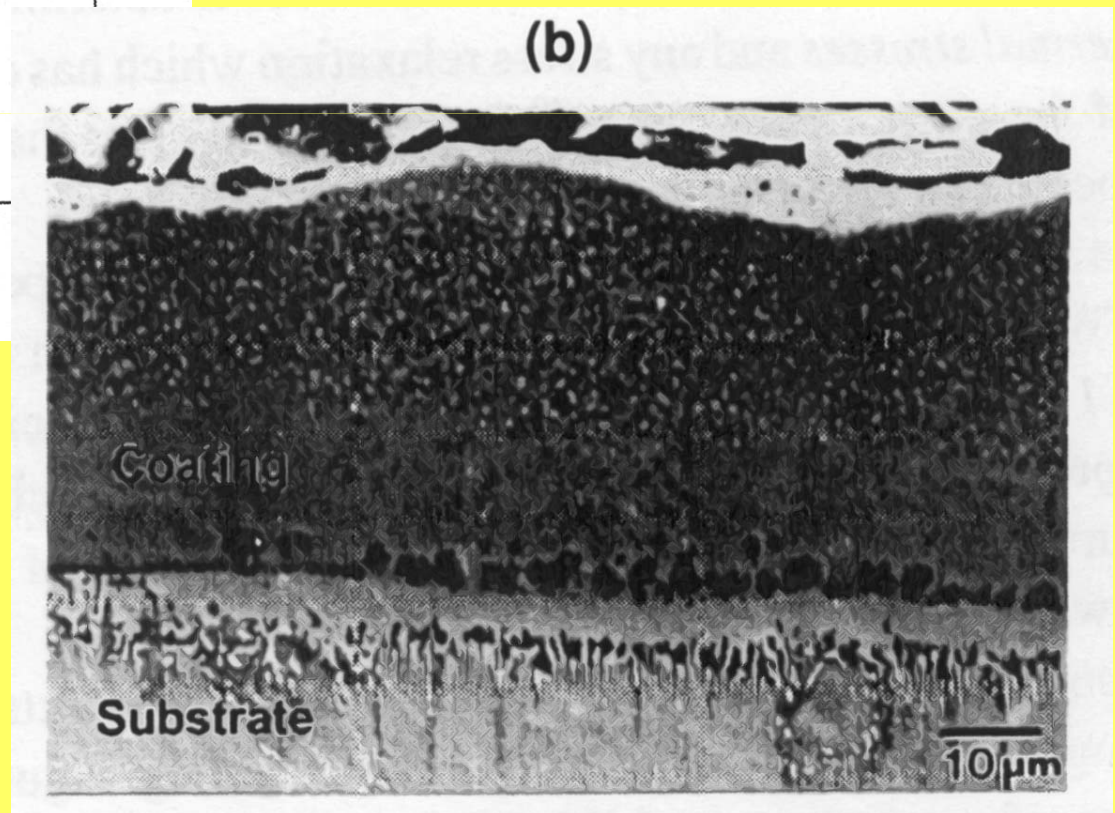
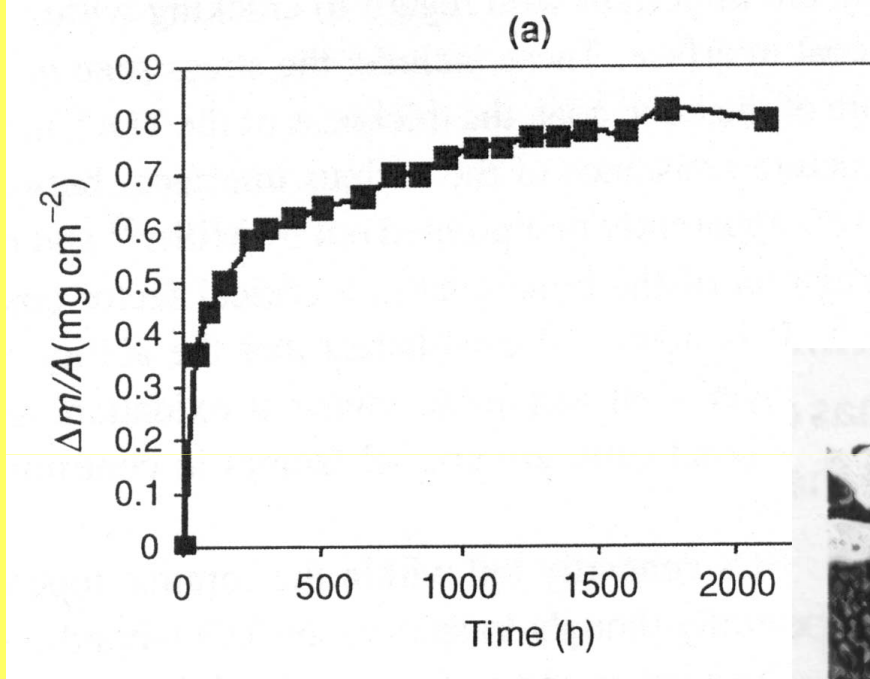
Micrograph of cross-section of a Ni-Co-Cr-Al-Y coating on a single-crystal Ni-base superalloy after 1000 one-hour cycles at 1100°C in air



Cyclic oxidation data for a straight aluminide and a platinum aluminide on IN-738 at 1200°C in air



Cyclic oxidation data for a sputtered Ti-Cr-Al coating on γ -TiAl at 900°C and the cross-section of coating after exposure

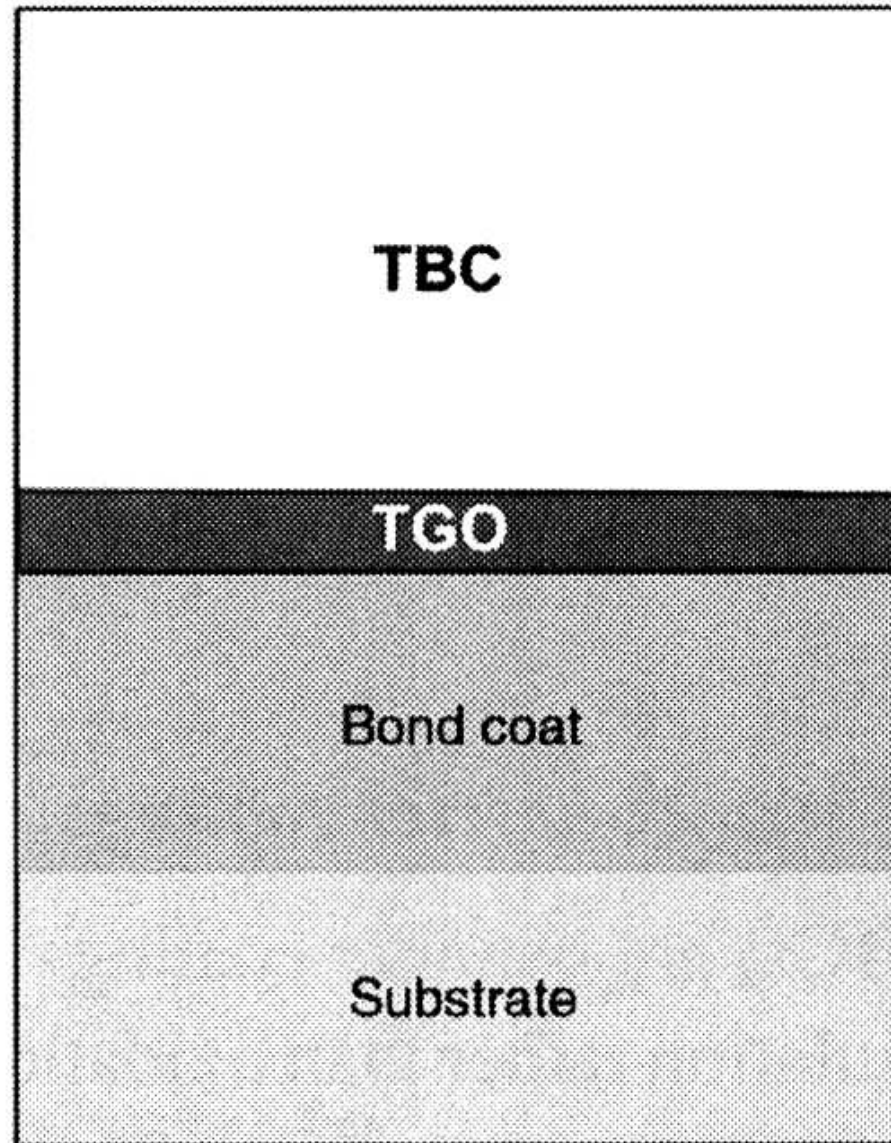


Thermal barrier coatings (TBC)

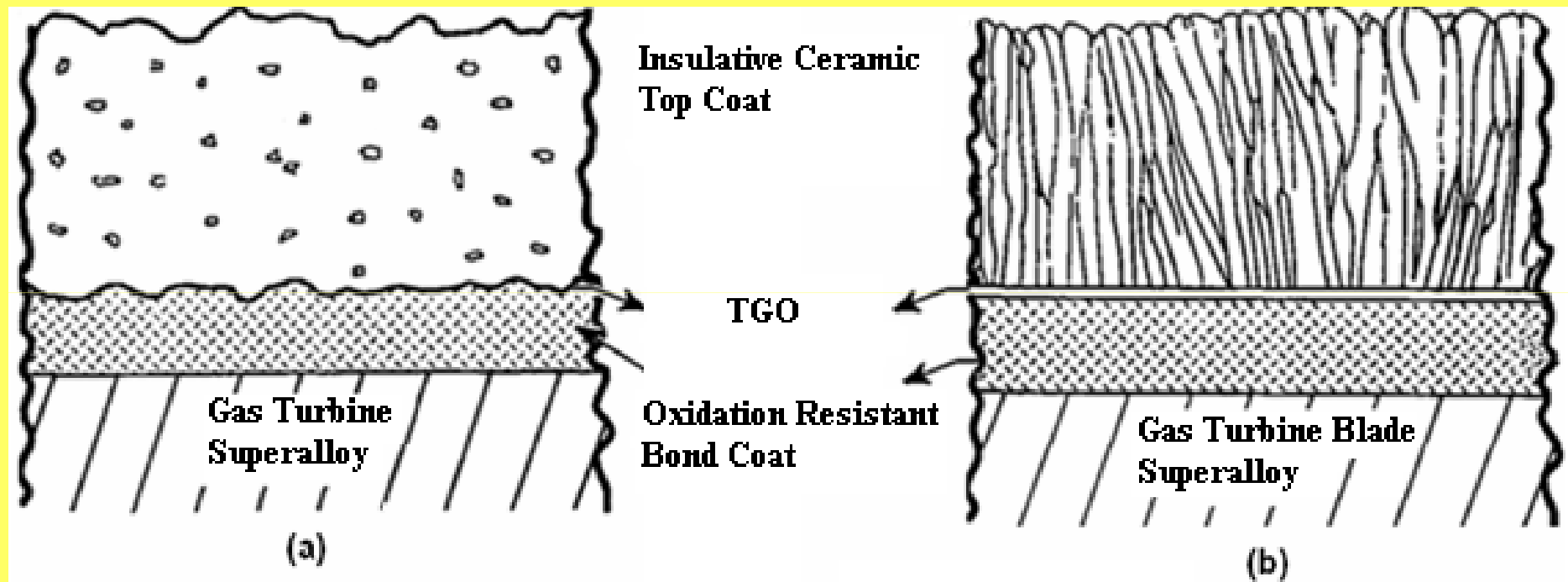
Thermal barrier coatings (TBC) are highly advanced materials systems usually applied to metallic surfaces, such as on gas turbine or aero-engine parts, operating at elevated temperatures, as a form of *exhaust heat management*.

These coatings serve to insulate components from large and prolonged heat loads by utilizing thermally insulating materials which can sustain an appreciable temperature difference between the load-bearing alloys and the coating surface. TBC coatings can allow for higher operating temperatures while limiting the thermal exposure of structural components, extending part life by reducing oxidation and thermal fatigue. In conjunction with active film cooling, TBCs permit working fluid temperatures higher than the melting point of the metal airfoil in some turbine applications.

Scheme of a typical TBC system

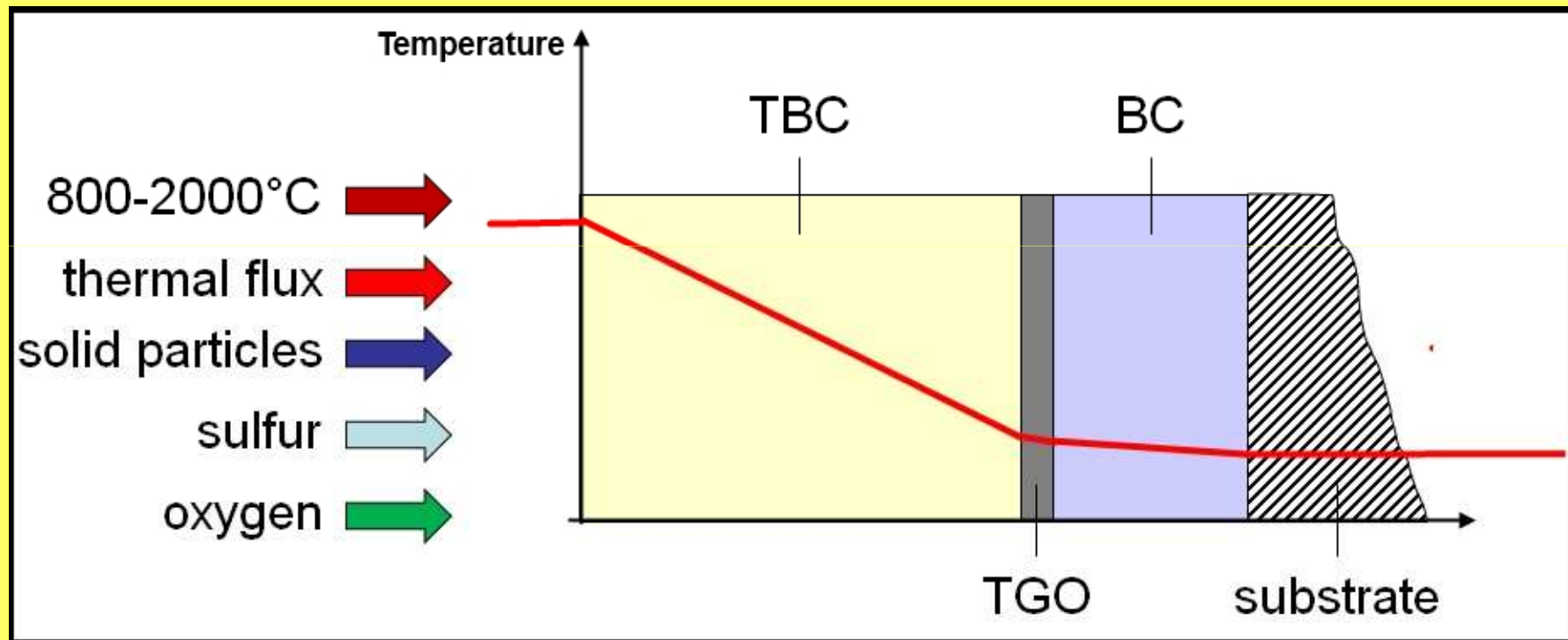


Scheme of a typical TBC system

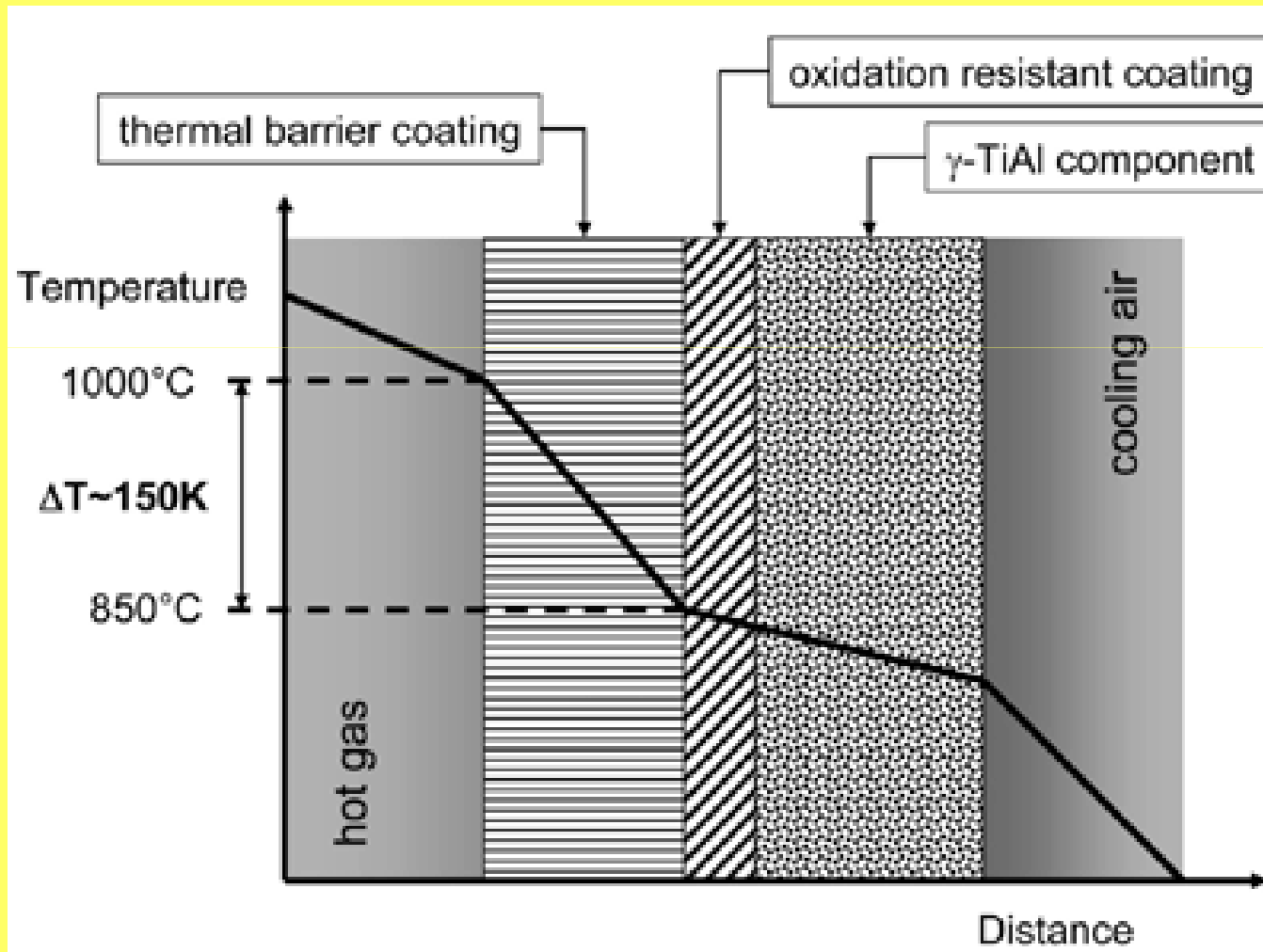


a) before and b) after oxidation

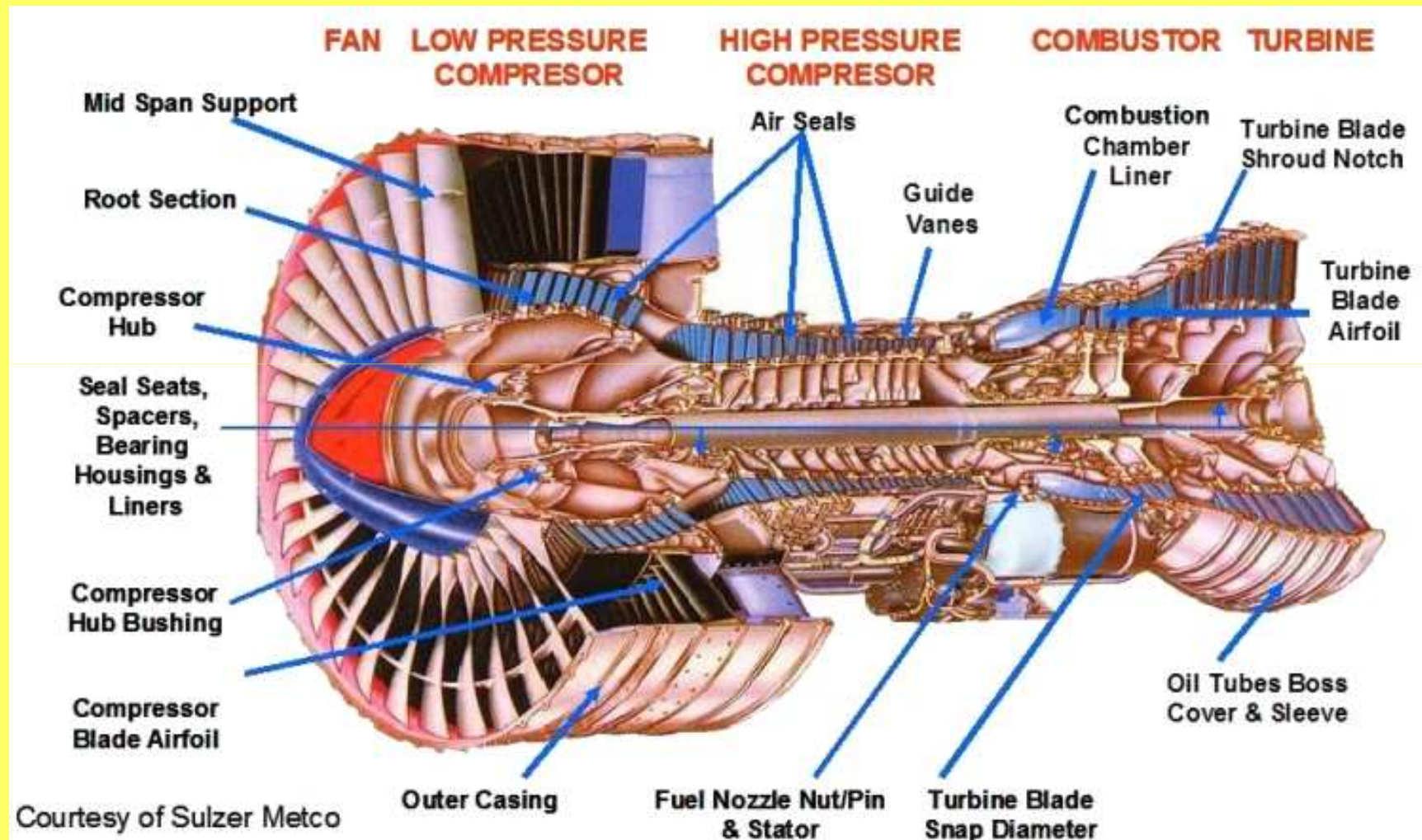
Scheme of the structure of a thermal barrier coating with a temperature profile



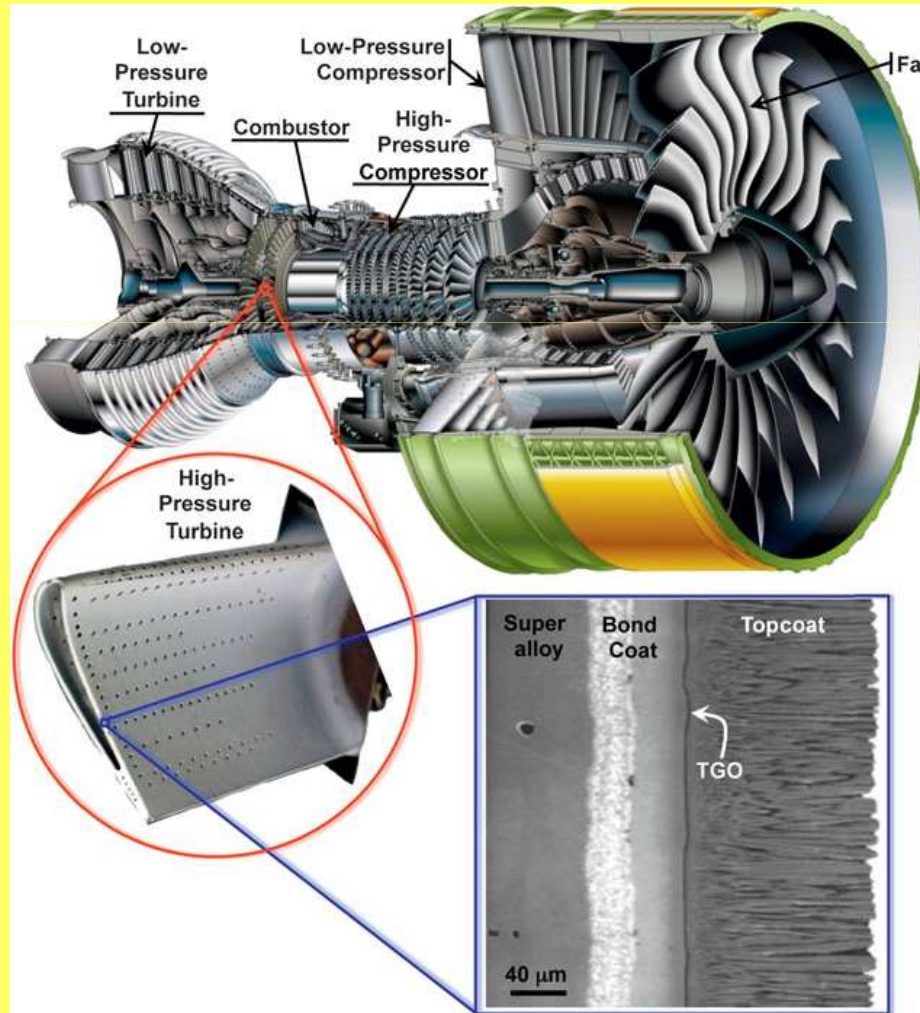
Scheme of the structure of a thermal barrier coating with a temperature profile



The parts of an aircraft engine using a plasma spray coating

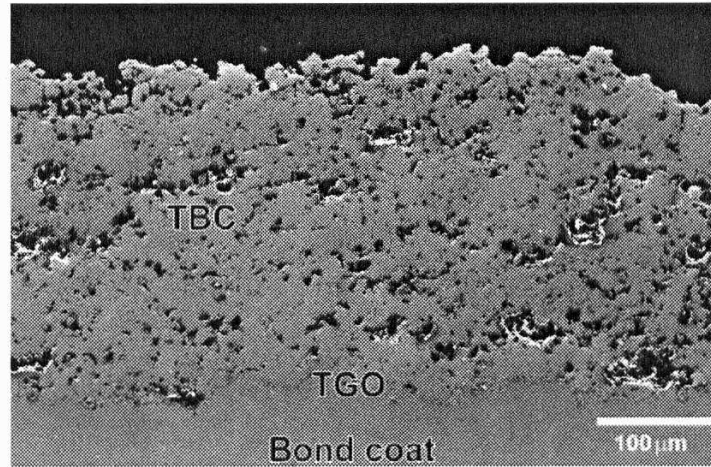


View of Engine Alliance GP7200 aircraft engine with photograph of a turbine blade (~ 10 cm long) with thermal-barrier coating (TBC) from the high-pressure hot section of an engine, and a scanning electron microscope (SEM) image of a cross-section of an electron beam physical vapor deposited 7 wt% yttria-stabilized zirconia TBC.

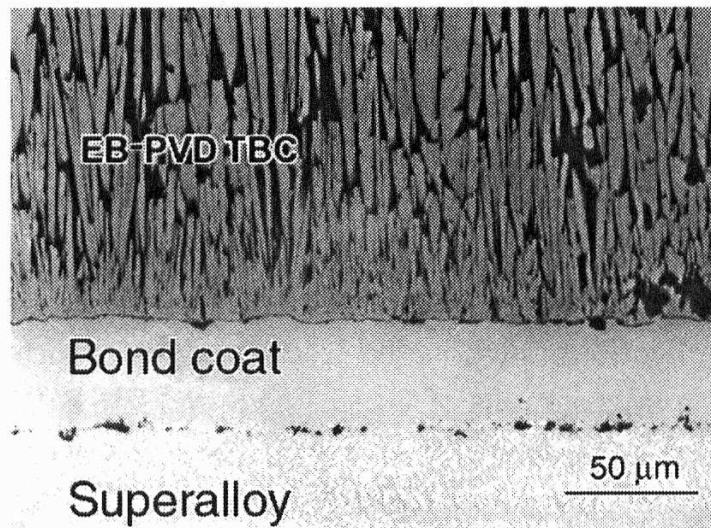


Cross-sections of TBC coatings

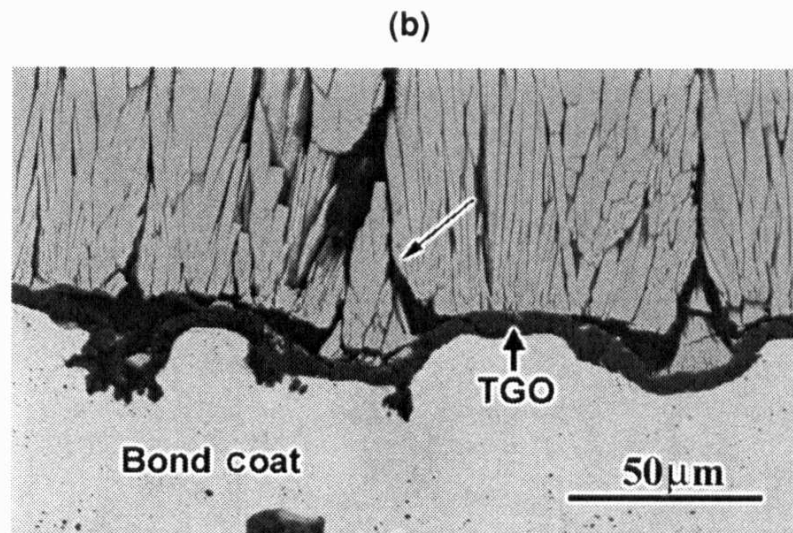
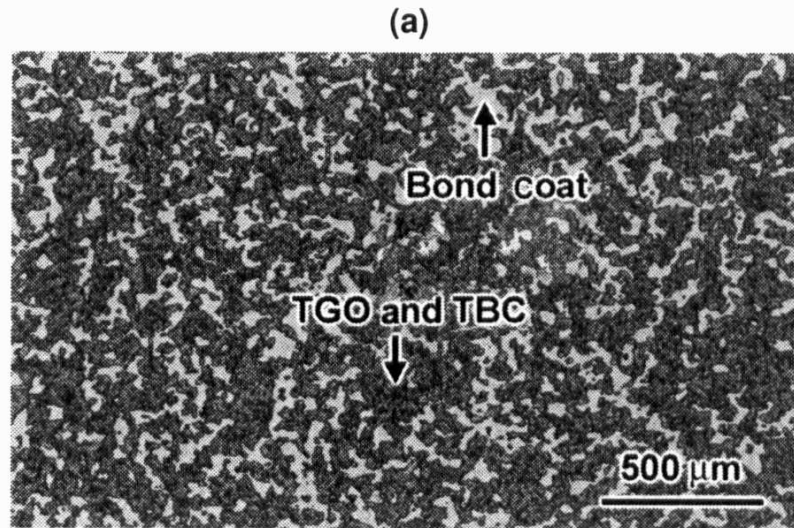
(a)



(b)



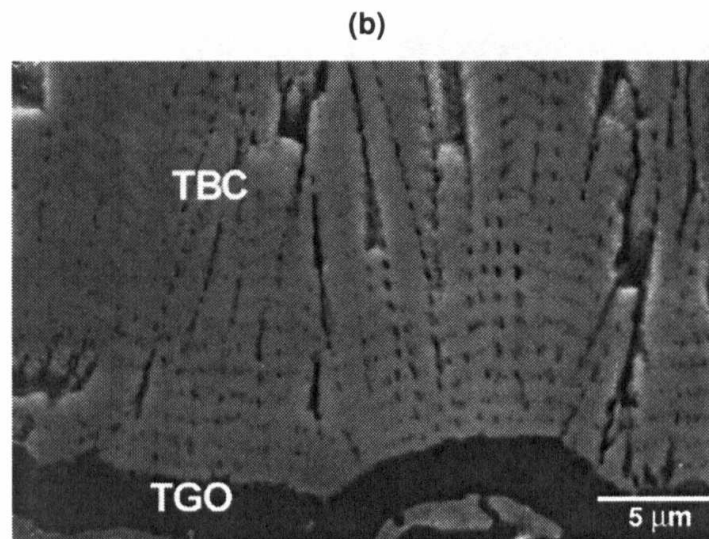
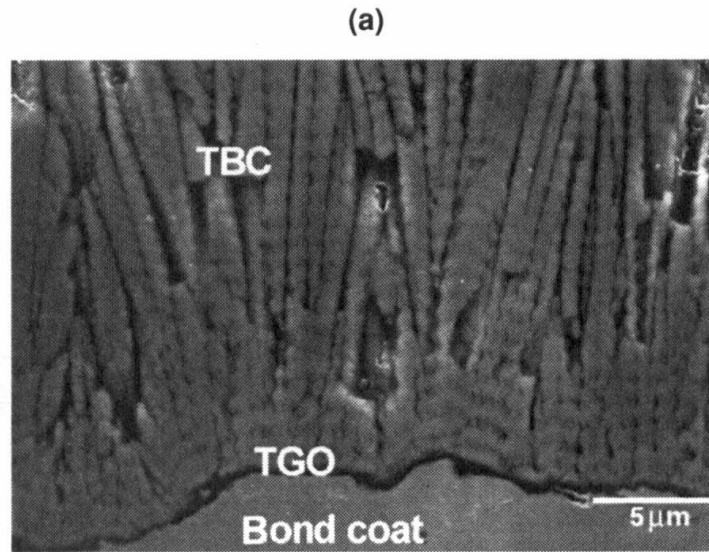
Surface and cross-sections of a layer of TBC protective coating after oxidation



EB-PVD YSZ TBC

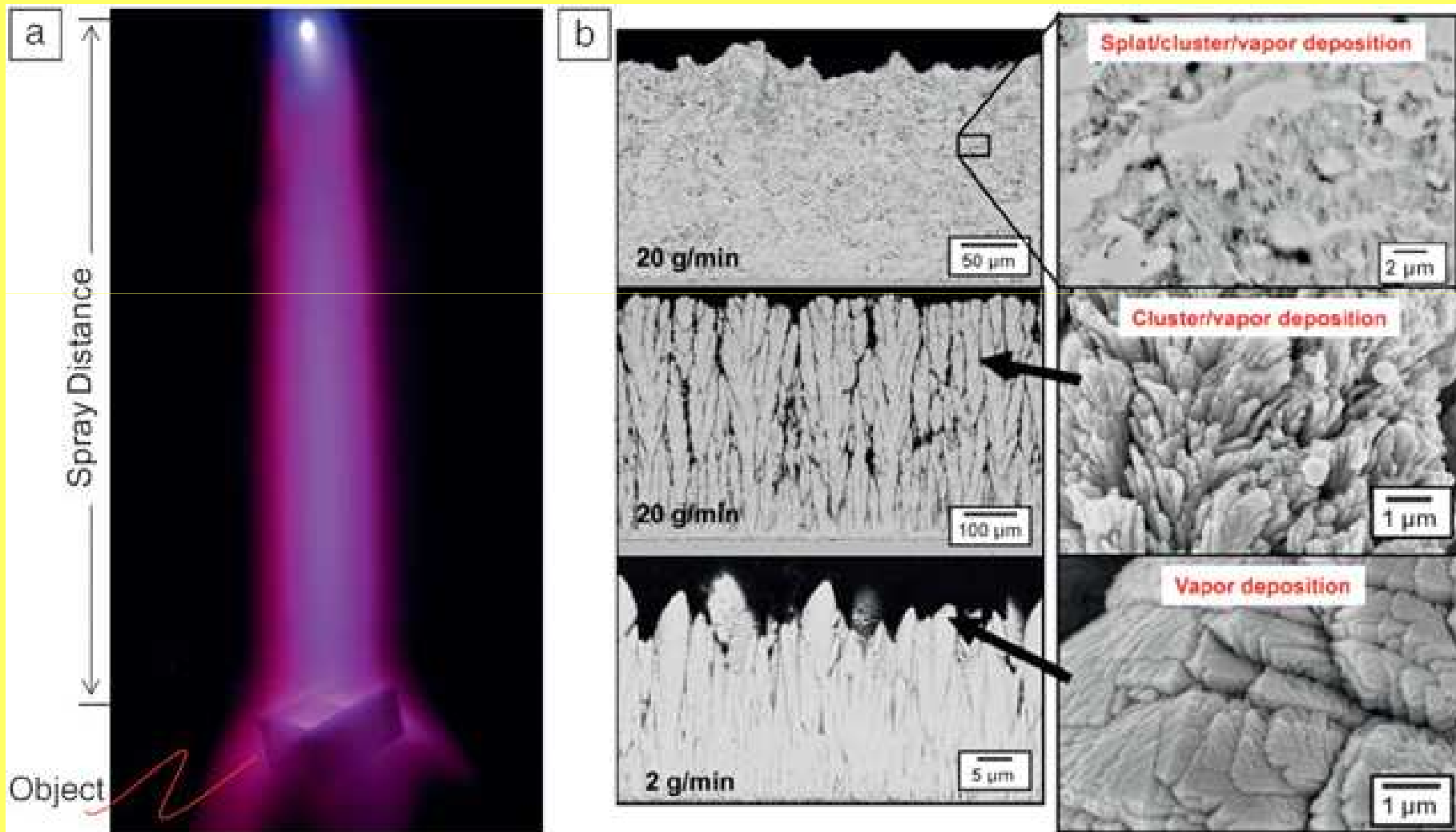
Pt-modified bond coat

Cross sections of a layer of TBC protective coating after oxidation

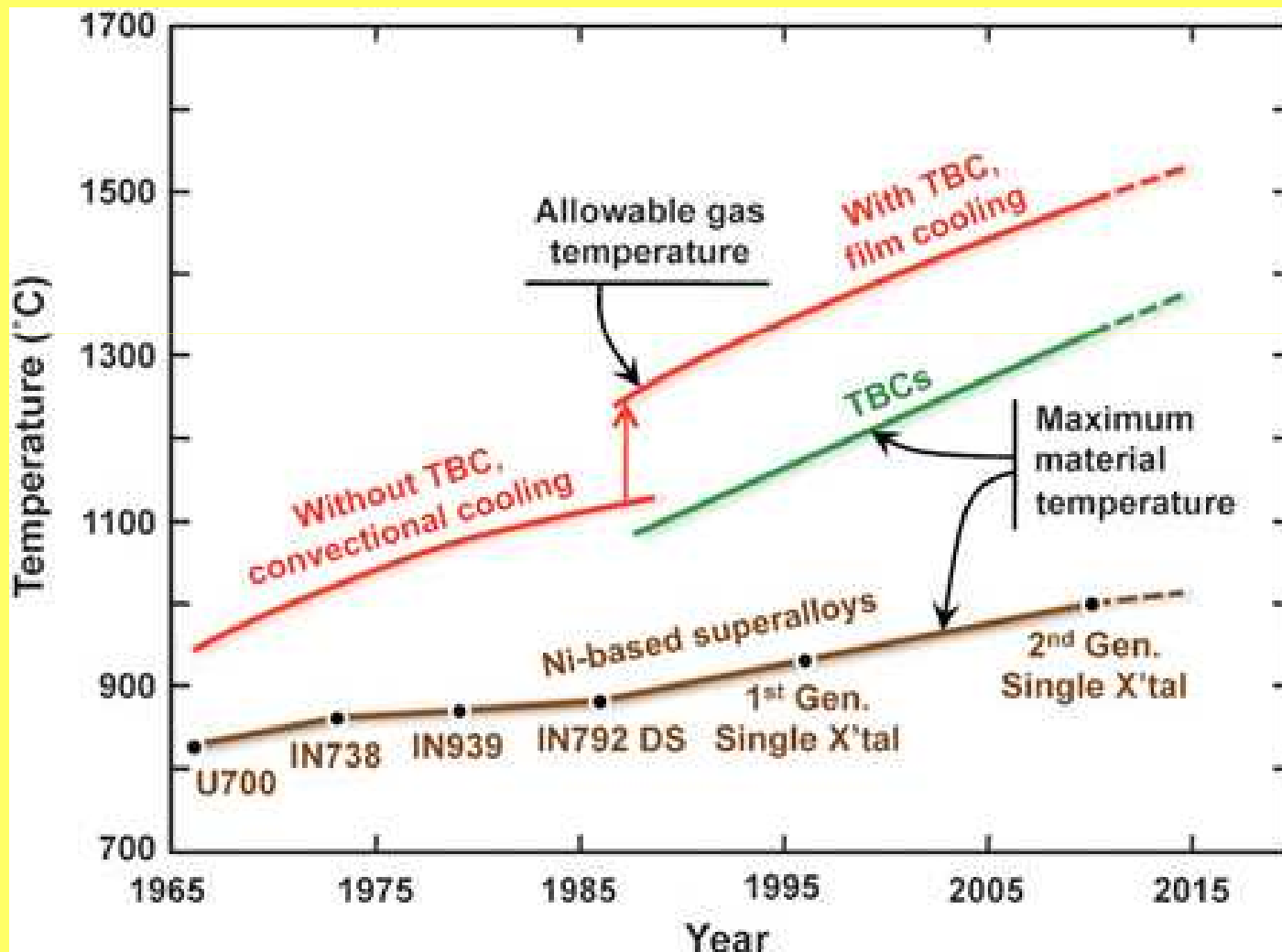


EB-PVD YSZ TBC

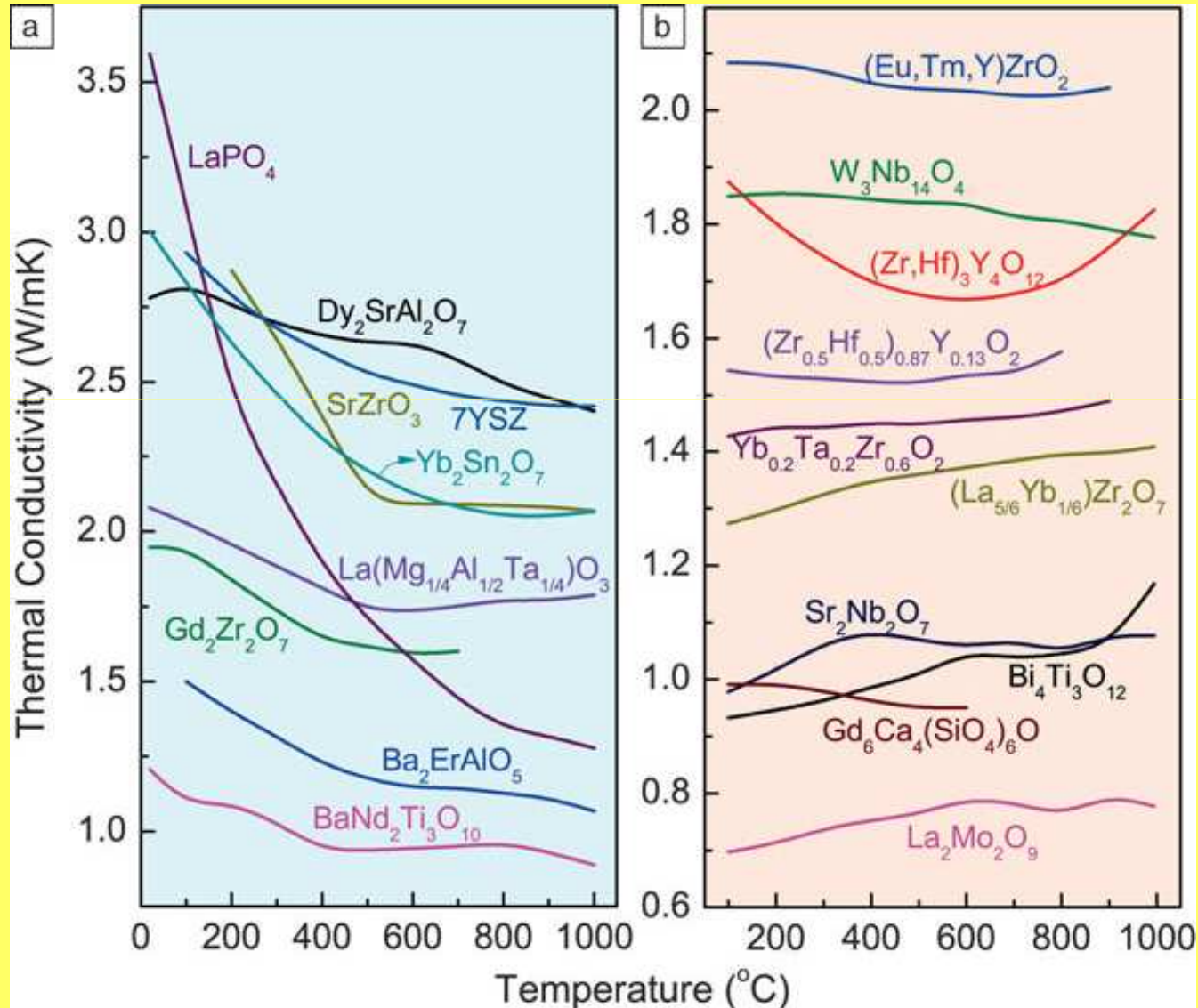
Photograph of a plasma spray physical vapor deposition (PSPVD) plume coating (a) and (b) scanning electron microscopy images of PSPVD microstructures from splat/cluster deposition all the way to vapor deposition obtained at different deposition rates



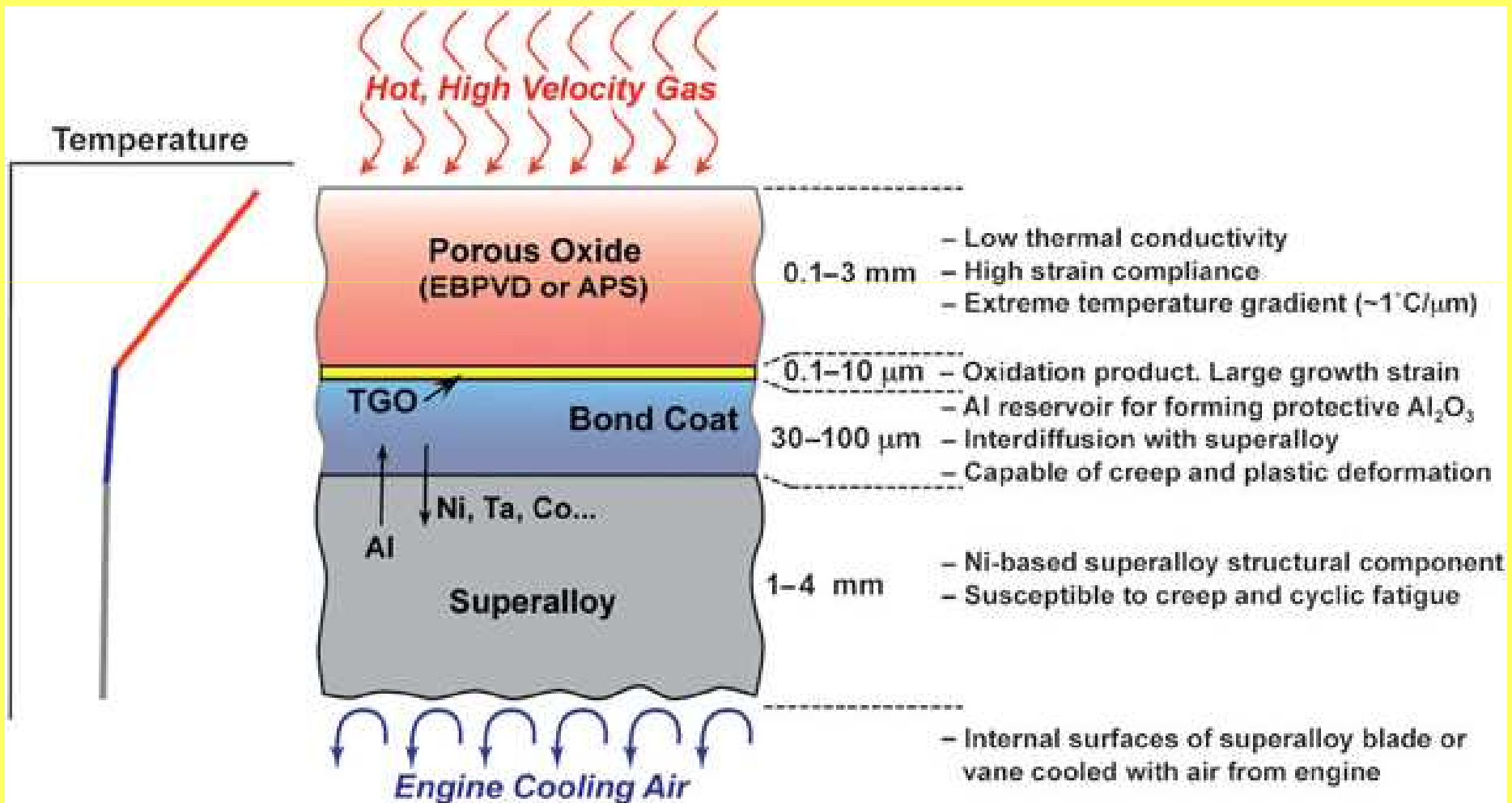
Progression of temperature capabilities of Ni-based superalloys and thermal-barrier coating (TBC) materials over the past 50 years. The red lines indicate progression of maximum allowable gas temperatures in engines, with the large increase gained from employing TBCs.



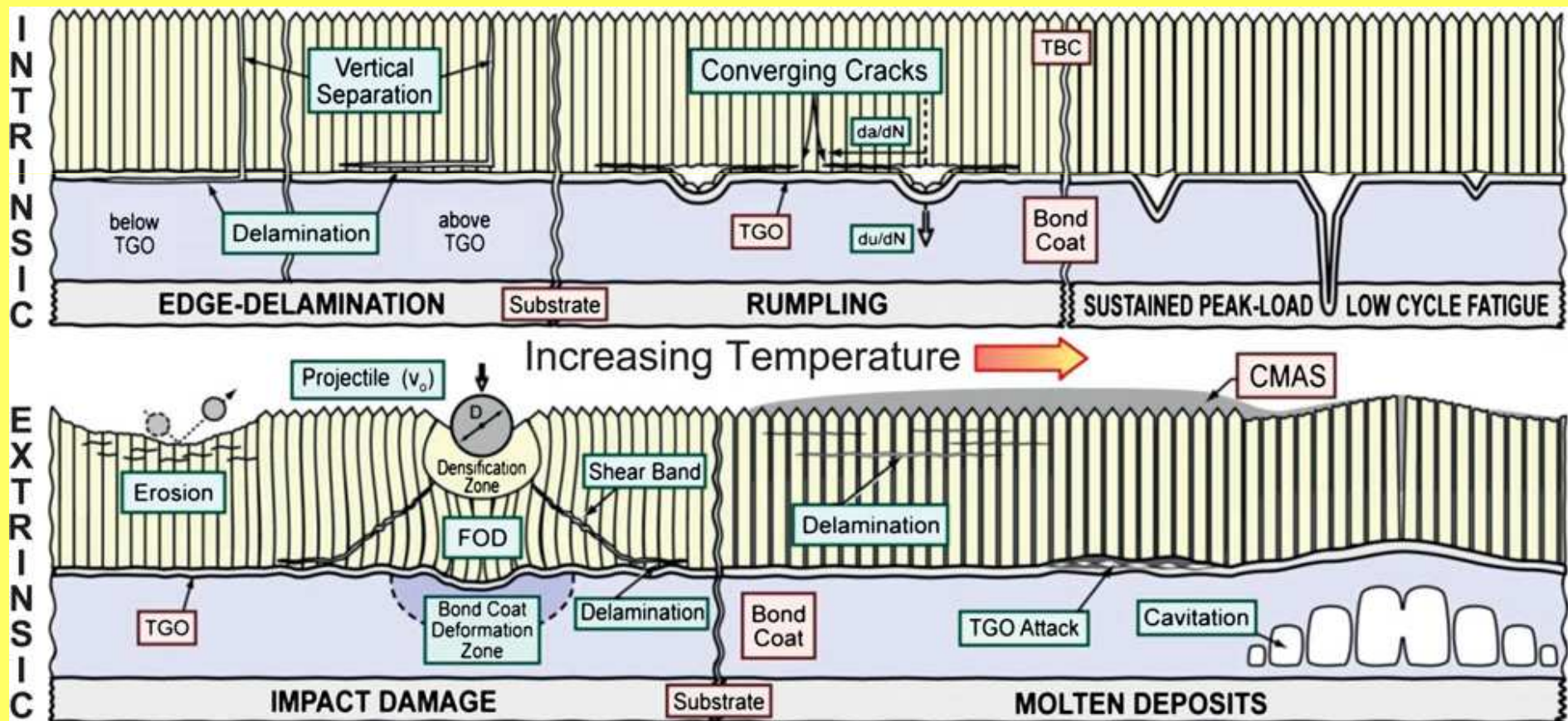
Thermal conductivity summary of the emerging ceramics for thermal-barrier coatings, whose conductivities vary with temperature (a) and temperature-independent thermal conductivities of ceramics (b)



Schematic illustration of the multilayer, multifunctional nature of the thermal barrier coating system. The ceramic topcoat is deposited by electron beam physical vapor deposition (EBPVD) or air plasma-spraying (APS).

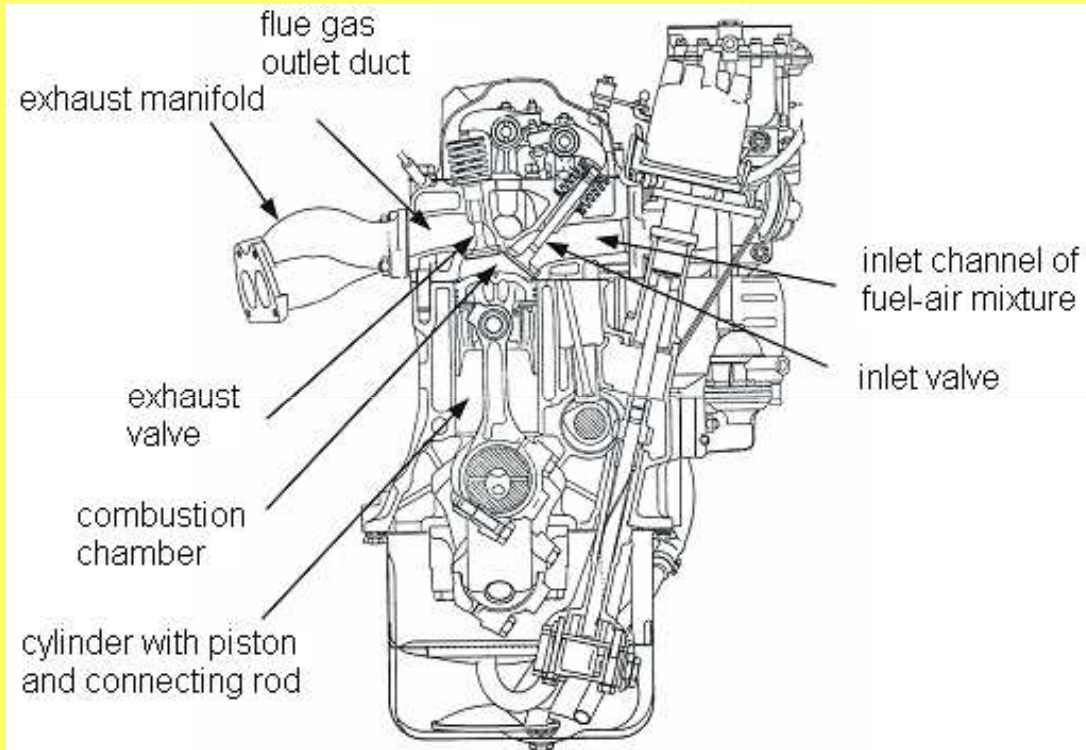


Failure mechanisms typical of current thermal-barrier coatings (TBCs): delamination cracks propagating through the TBC, chemical attack of the thermally grown oxide (TGO) with concomitant loss of adherence, creep cavitation of the bond coat below a heavily penetrated TBC



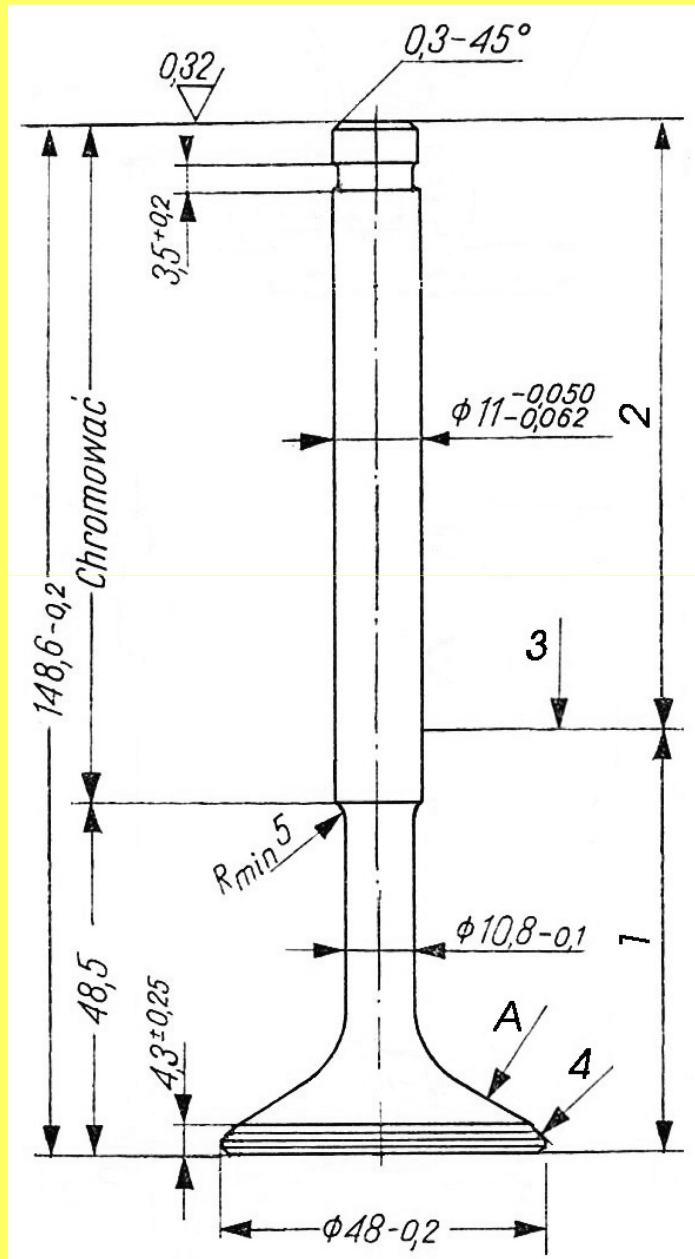
Thermal barrier coatings in automobiles

Cross section of four-cylinder in-line engine with spark ignition, Fiat



M. Bernhardt, S. Dobrzyński, E. Loth, *Silniki samochodowe*,
Wydawnictwo Komunikacji i Łączności, Warszawa, 1988, s.327

Construction of an exhaust valve

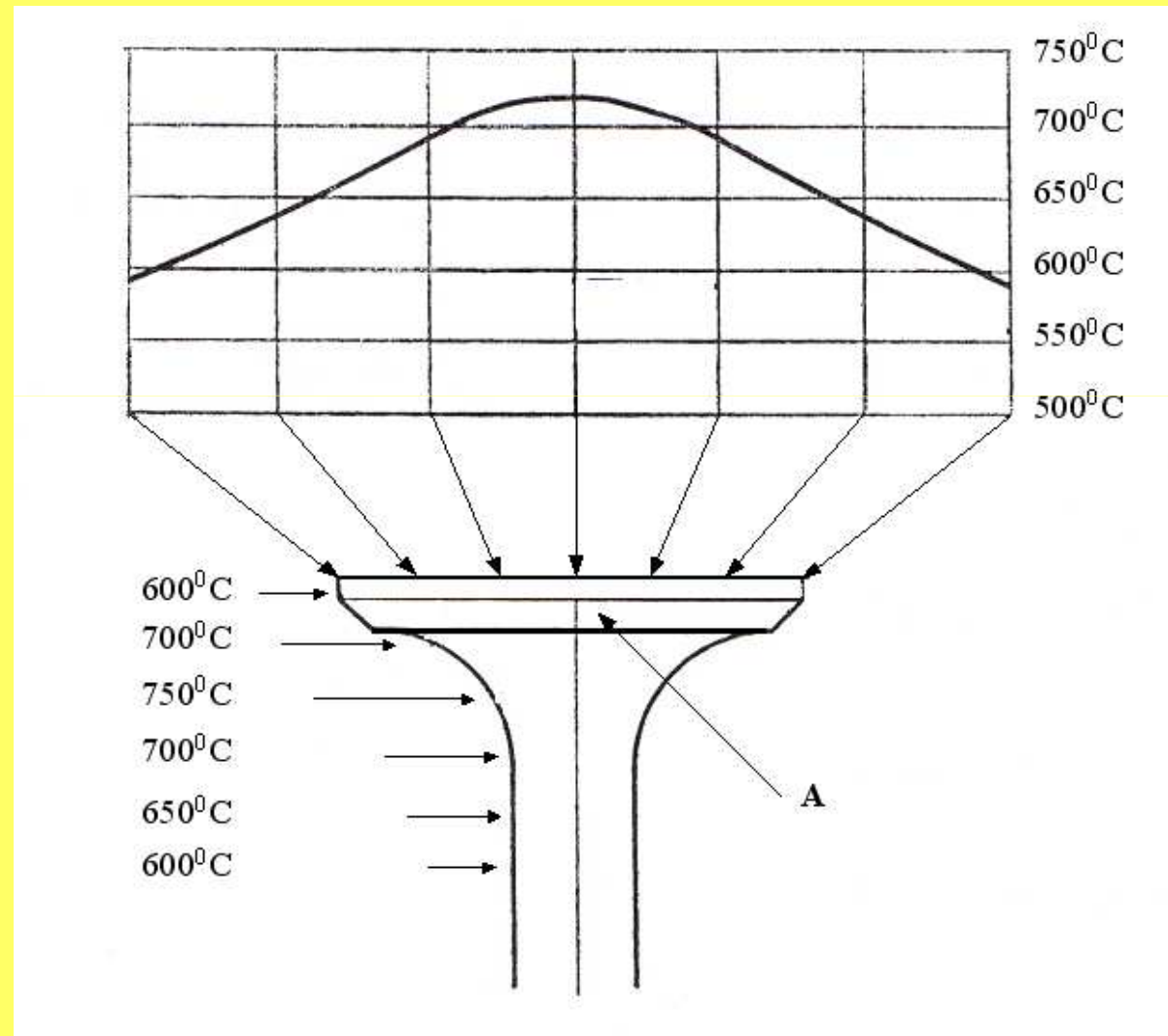


- 1 – mushroom - austenitic steel Cr-Ni-W-Mo in supersaturated and aged state,
- 2 – handle - Cr-Si-Mo steel thermally improved,
- 3 – place of friction welding,
- 4 – valve face hard coated of stellite Co-Cr-W

Working conditions of valves in car engines

- aggressive atmosphere of combustion gases
- high temperature ($T \approx 1173 \text{ K}$)
- rapid changes of temperature (thermal shocks)

Temperature distribution in the exhaust valve - petrol engine with spark ignition

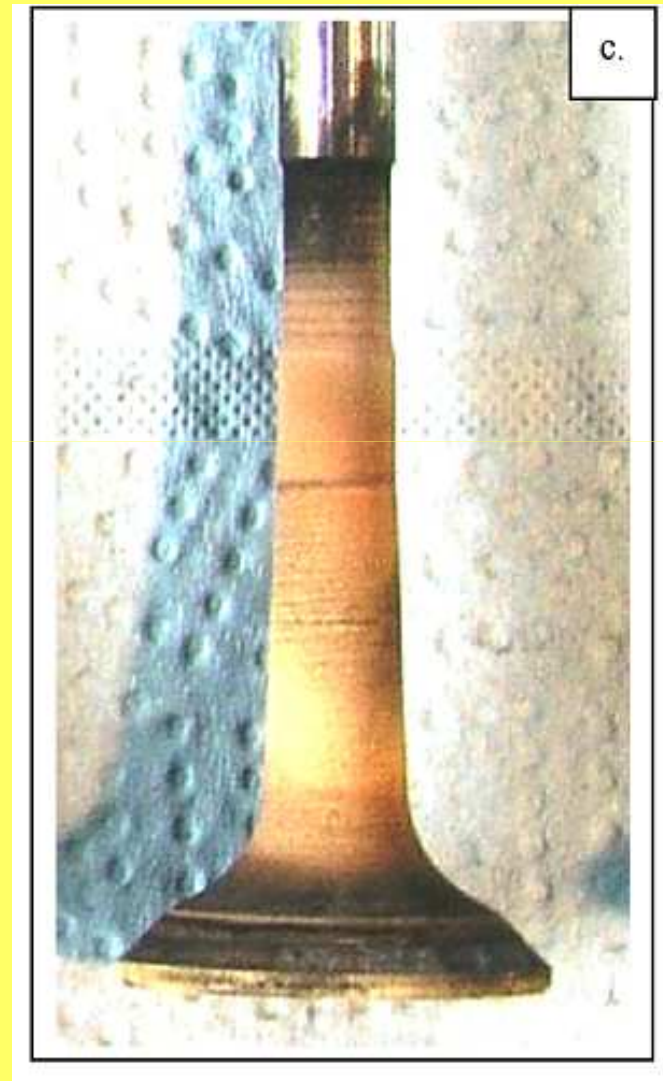


Chemical compositions of an engine gases with spark and spontaneous ignition (wt. %)

Components of exhaust gases	Units	Method of ignition		Toxicity evaluation
		spark ignition	spontaneous	
Nitrogen	% vol.	74-77	76-78	neutral
Oxygen	% vol.	0,3-8,0	2,0-18,0	as above
Water vapor	% vol.	3,0-5,5	0,4-5,0	as above
Carbon dioxide	% vol.	5,0-12,0	1,0-10,0	as above
Carbon monoxide	% vol.	5,0-10,0	0,01-0,5	toxic
Nitrogen oxides	% vol.	0,0-0,8	0,002-0,5	as above
Hydrocarbons	% vol.	0,2-3,0	0,009-3,0	as above
Aldehydes	% vol.	0,0-0,2	0,001-0,009	as above
Soot	g/m ³	0,0-0,04	0,01-1,1	as above
3,4 benzopyrene	g/m ³	to 15,0	to 10,0	carcinogenic

Merkisz J., *Ekologiczne problemy silników spalinowych Tom I i II.*
Wydawnictwo Politechniki Poznańskiej, Poznań 1999

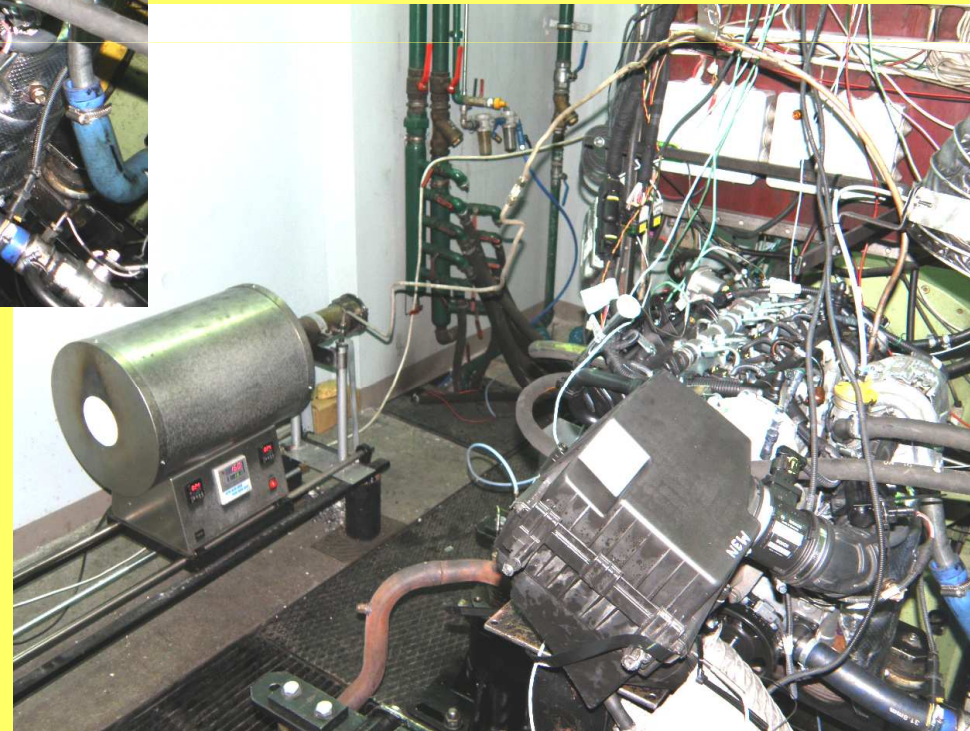
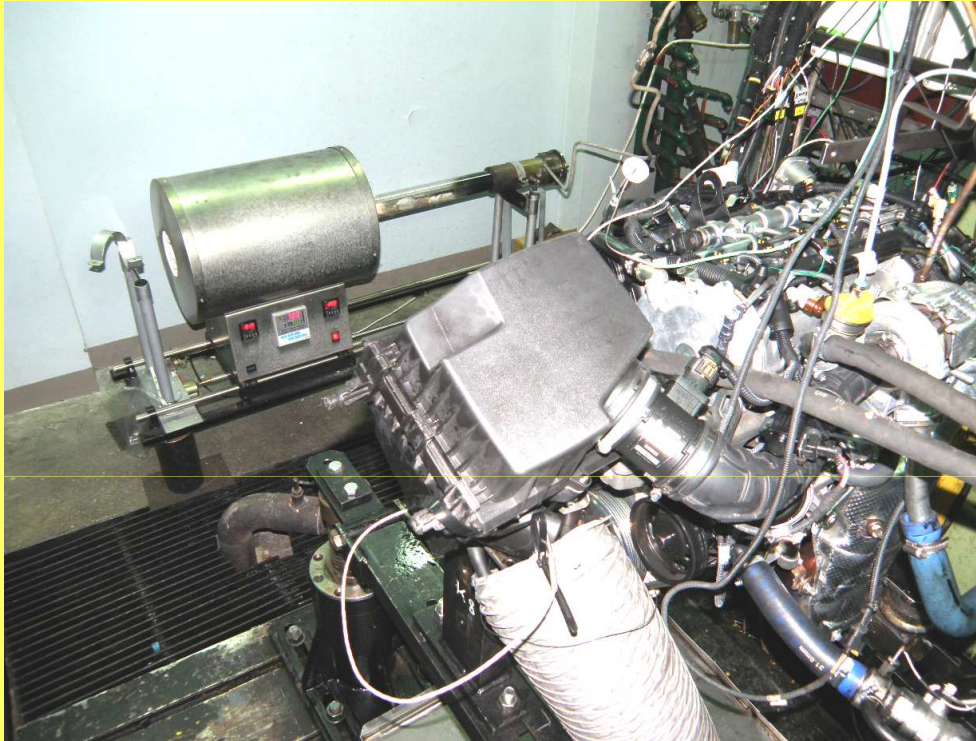
Exhaust valves after the 1000 hour test - engine with spontaneous ignition



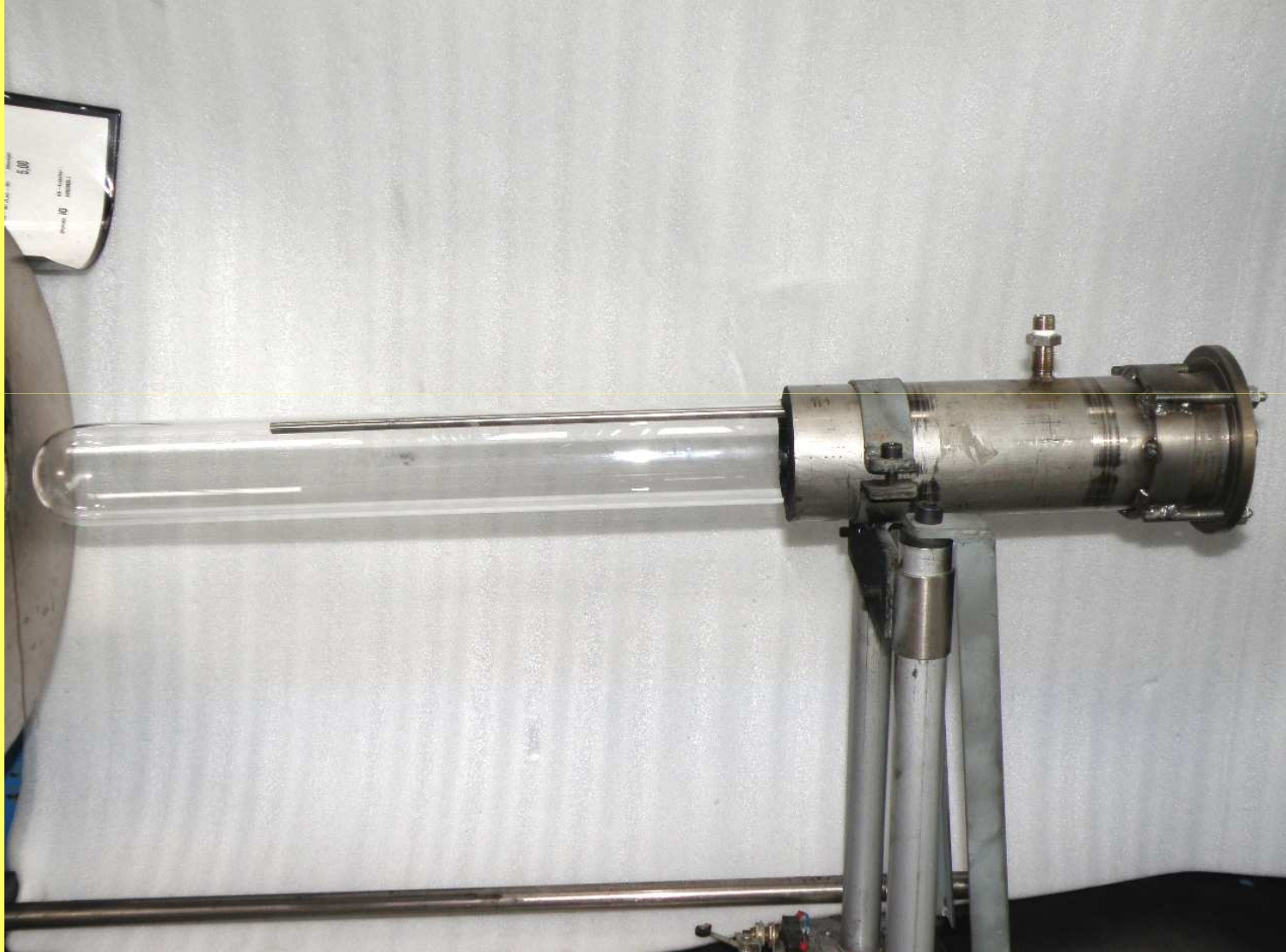
The chemical composition of valve steels (% wt.)

Type of steel	C	Mn	Si	Cr	Ni	N	W	Nb	S	P	Mo	Fe
X33CrNiMn23-8	0.35	3.3	0.63	23.4	7.8	0.28	0.02	-	<0.005	0.014	0.11	bal.
X50CrMnNiNbN21-9	0.54	7.61	0.30	19.88	3.64	0.44	0.86	2.05	0.001	0.031	-	bal.
X53CrMnNiN20-8	0.53	10.3	0.30	20.5	4.1	0.41	-	-	<0.005	0.04	0.12	bal.
X55CrMnNiN20-8	0.55	8.18	0.17	20.0	2.3	0.38	-	-	<0.005	0.03	0.11	bal.

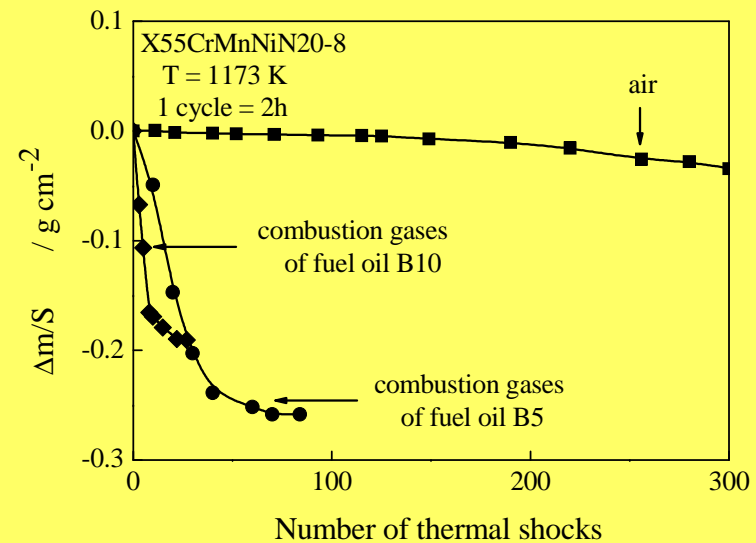
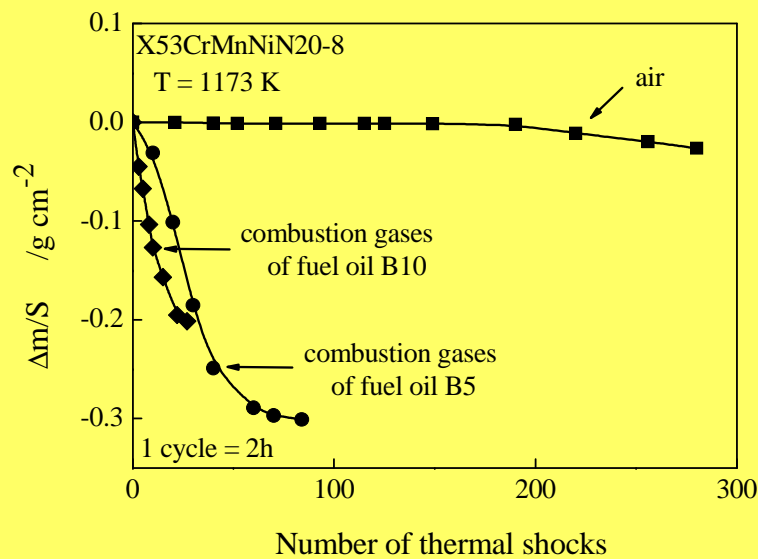
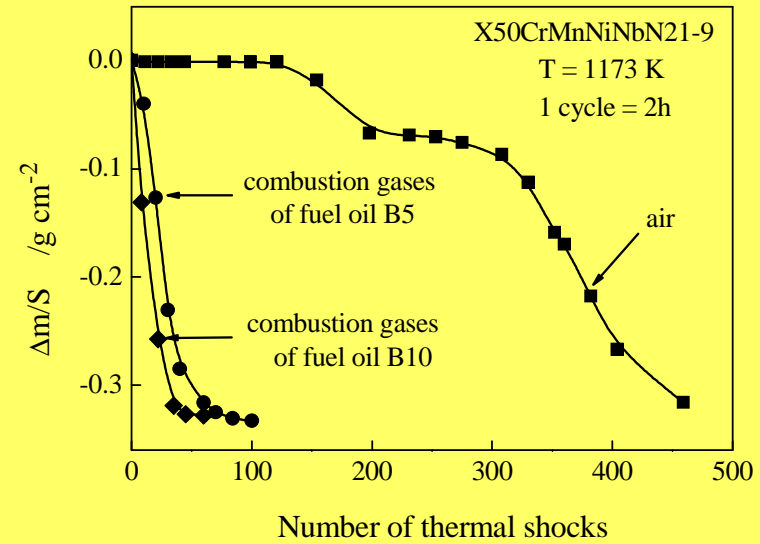
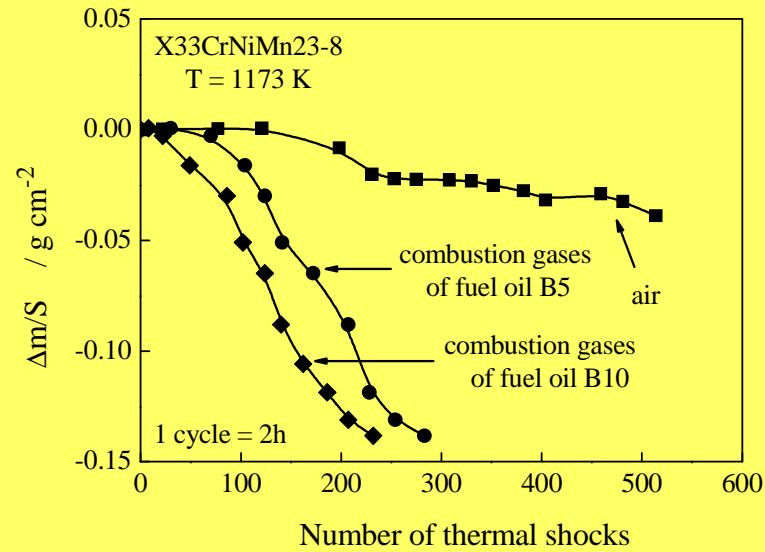
The corrosion test of valve steels under thermal shock conditions in engine house



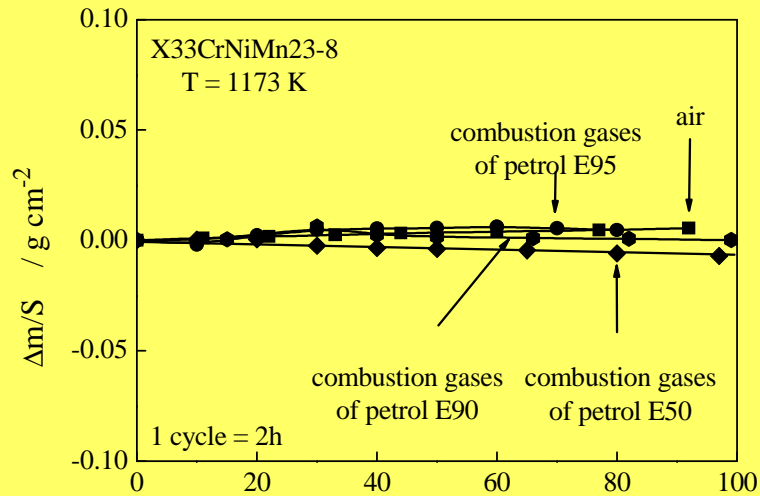
Hybrid reactive head



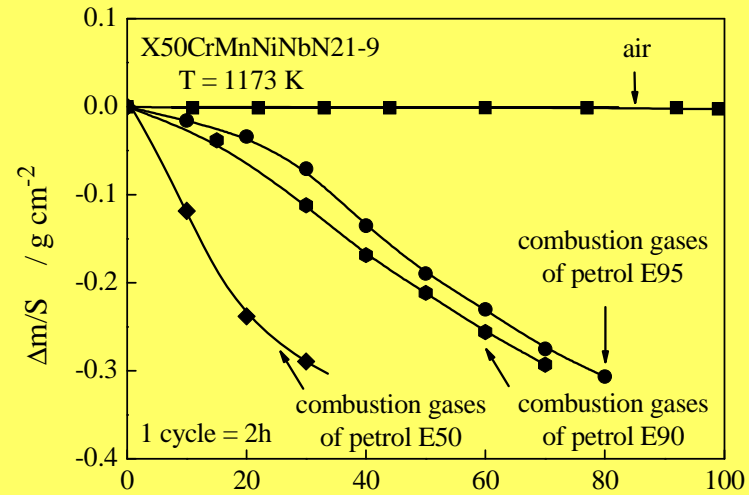
Corrosion kinetics of tested valve steels under thermal shock conditions



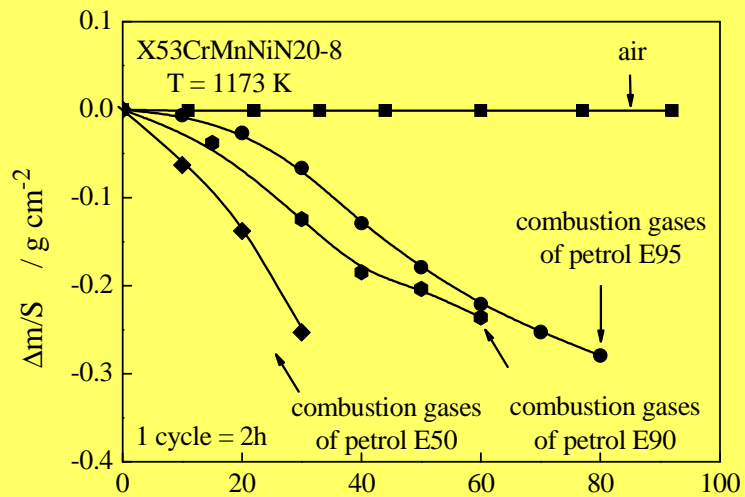
Corrosion kinetics of tested valve steels under thermal shock conditions



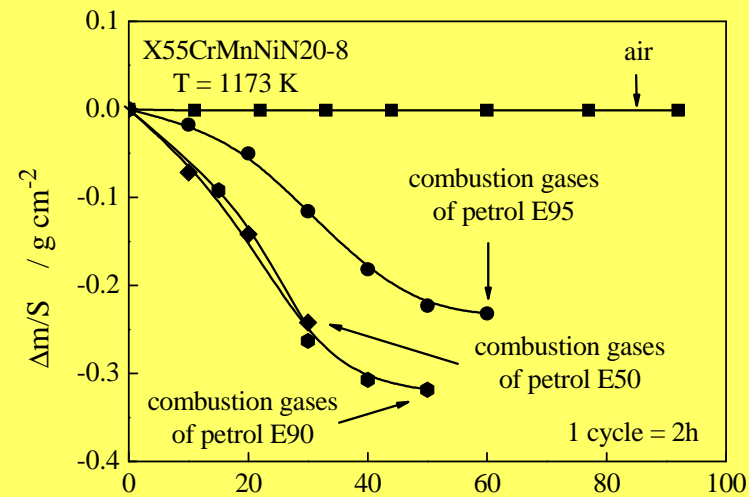
Number of thermal shocks



Number of thermal shocks

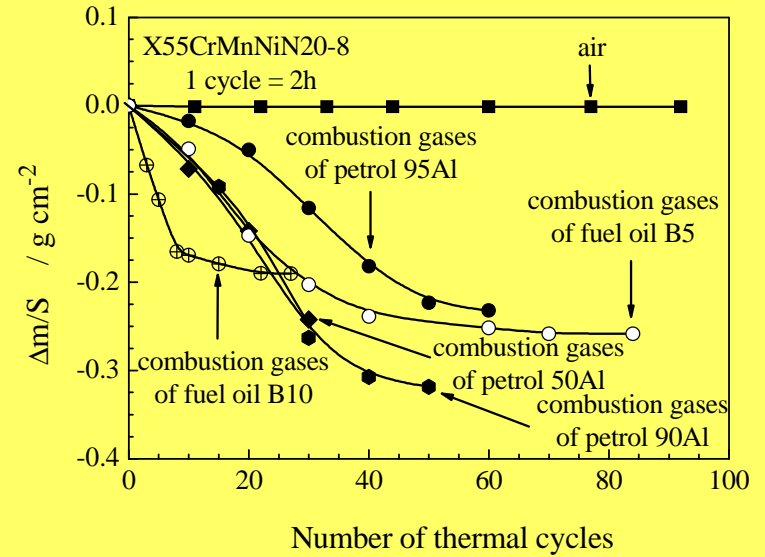
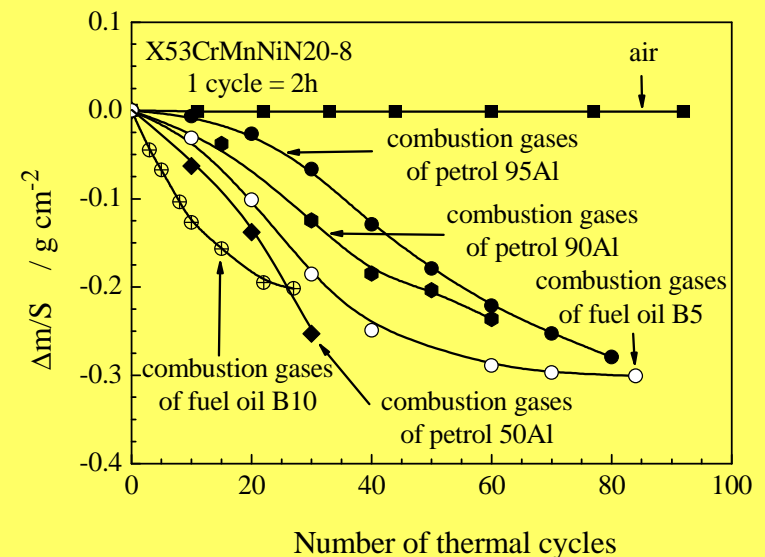
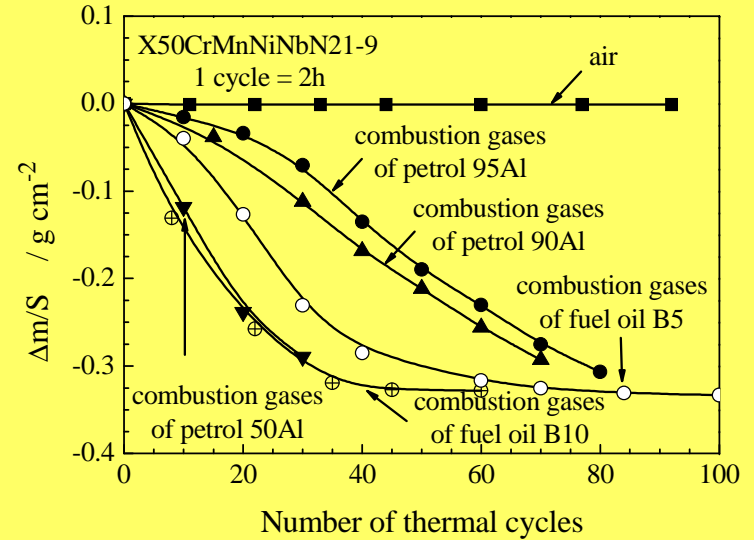
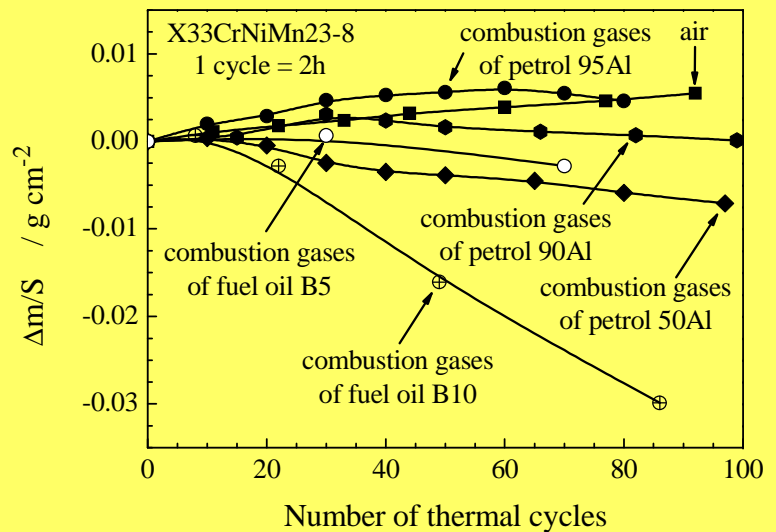


Number of thermal shocks

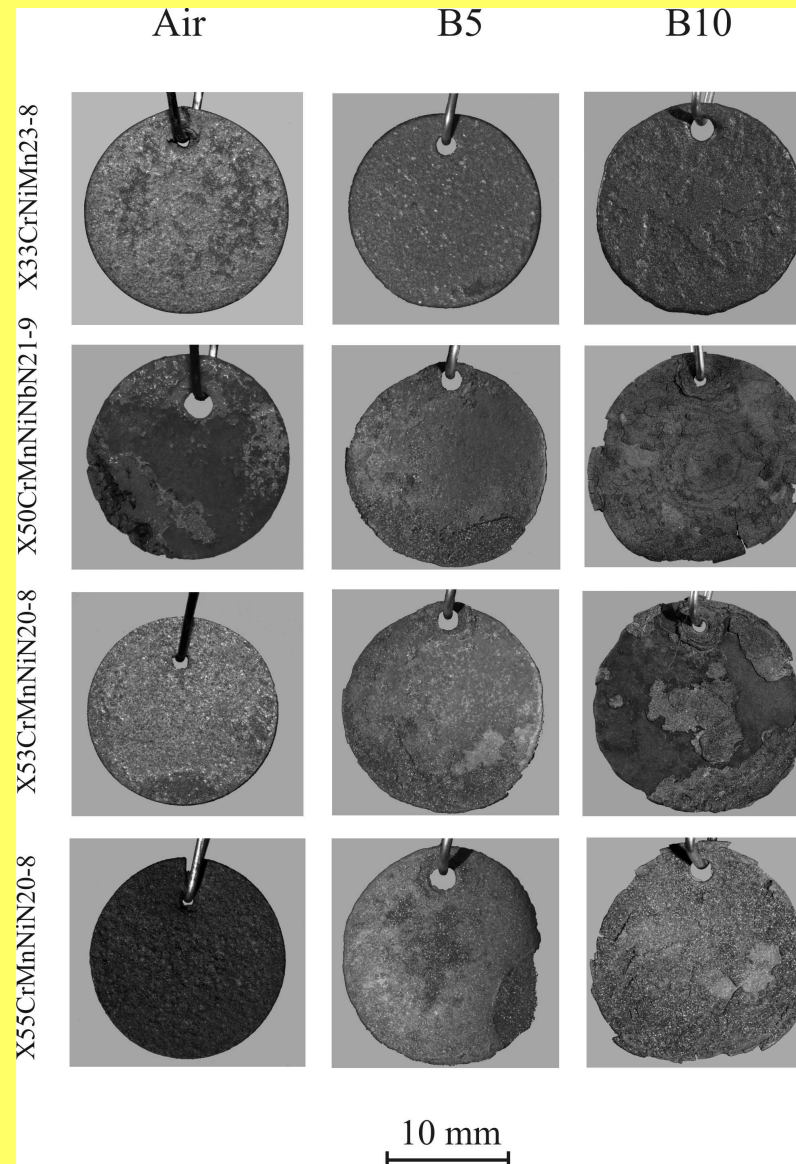


Number of thermal shocks

Comparison of corrosion kinetics of valve steels under thermal shock conditions at different atmospheres

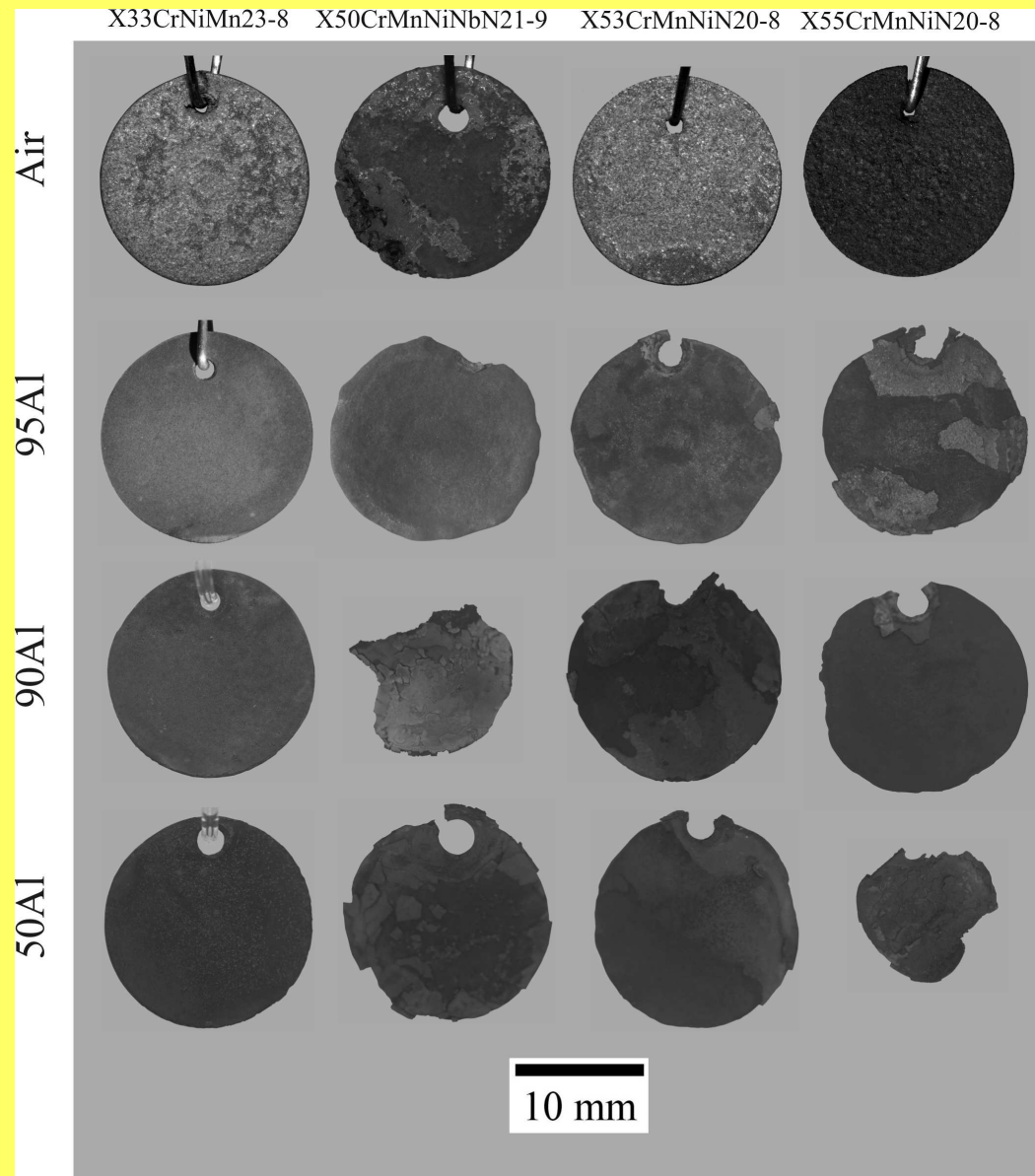


Images of valve steel samples corroded under thermal shock conditions in a number of aggressive atmospheres

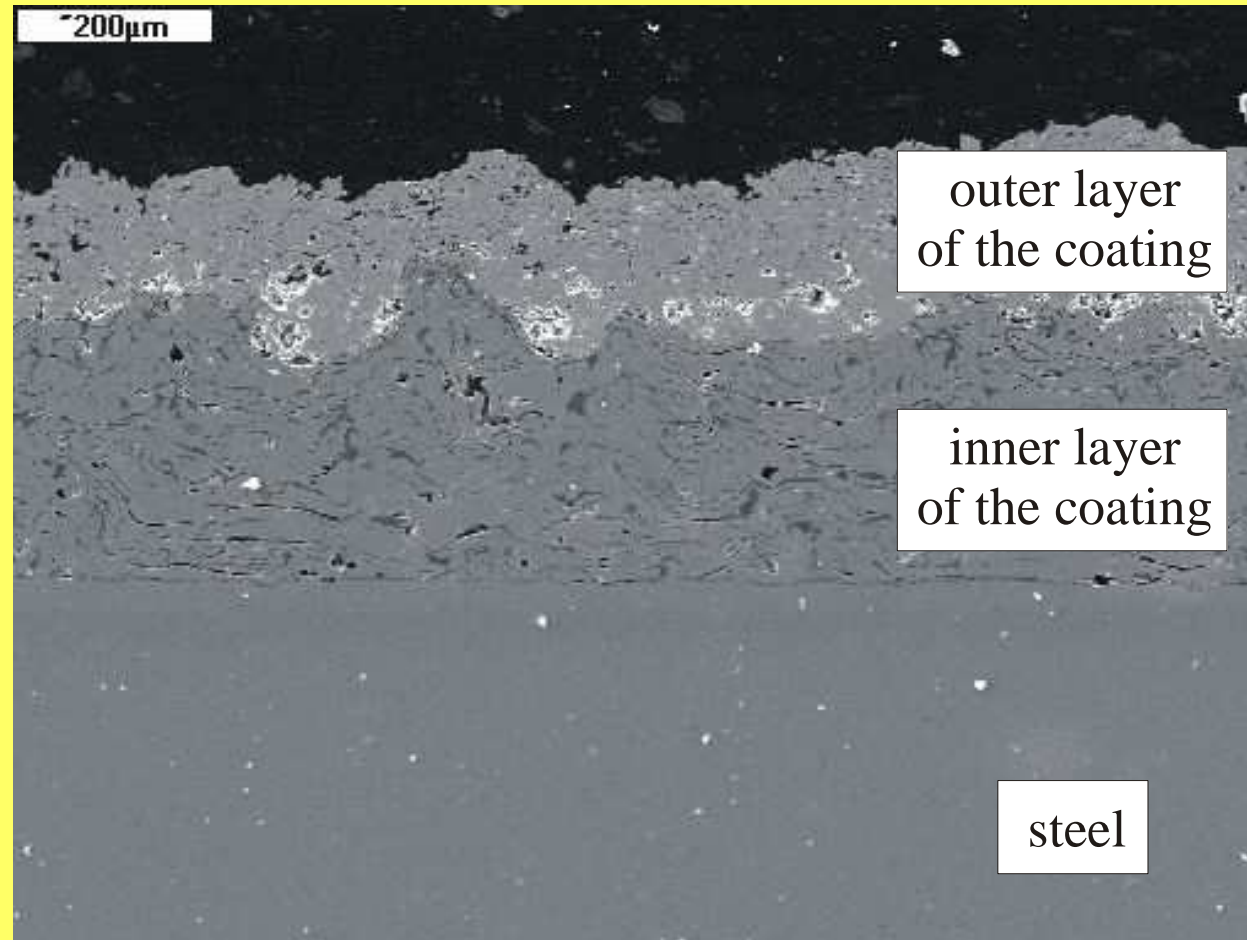
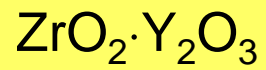


T = 1173K

Images of valve steel samples corroded under thermal shock conditions in a number of aggressive atmospheres



Cross-section of valve steel covered by protective coating
with TBC layer

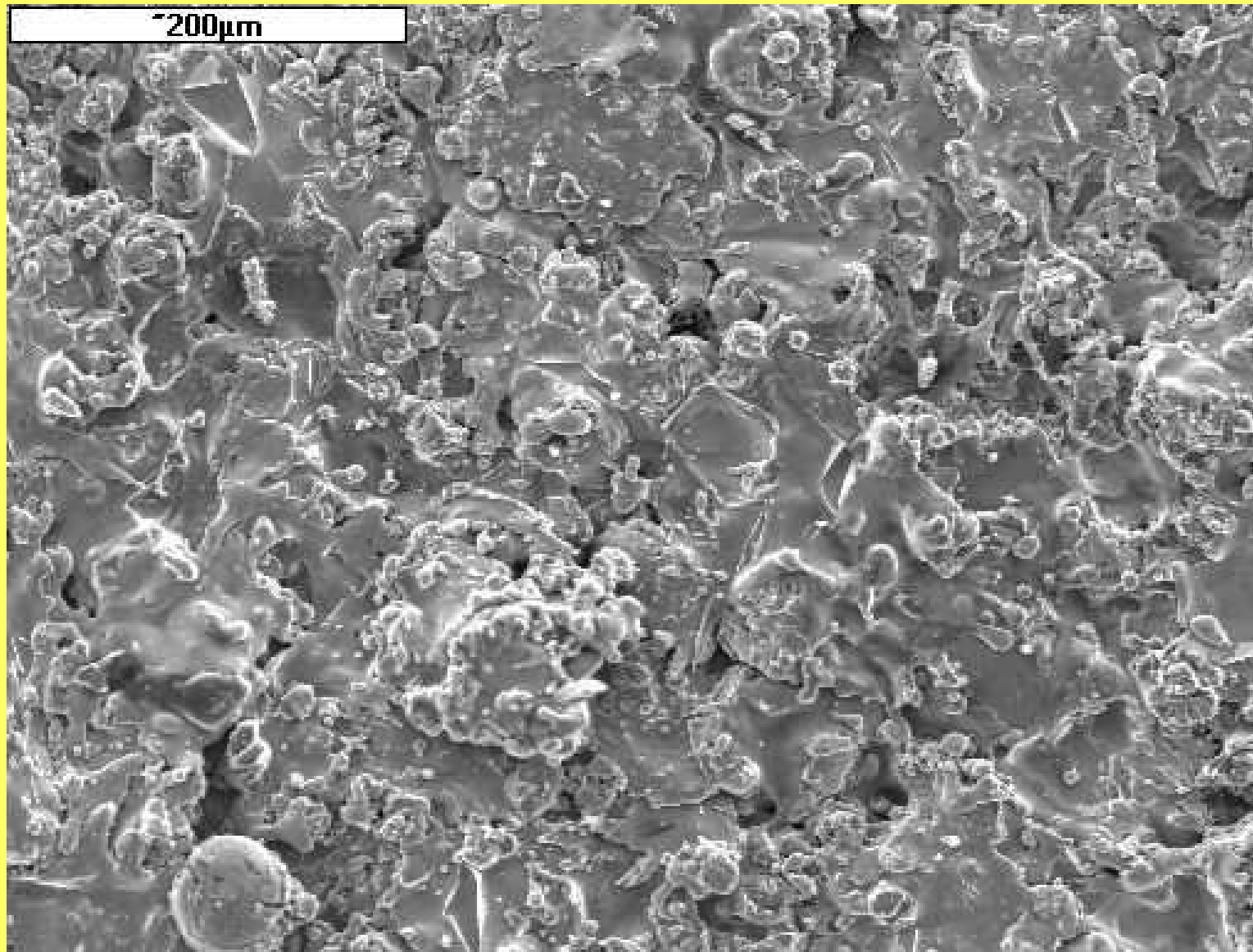


outer layer
of the coating

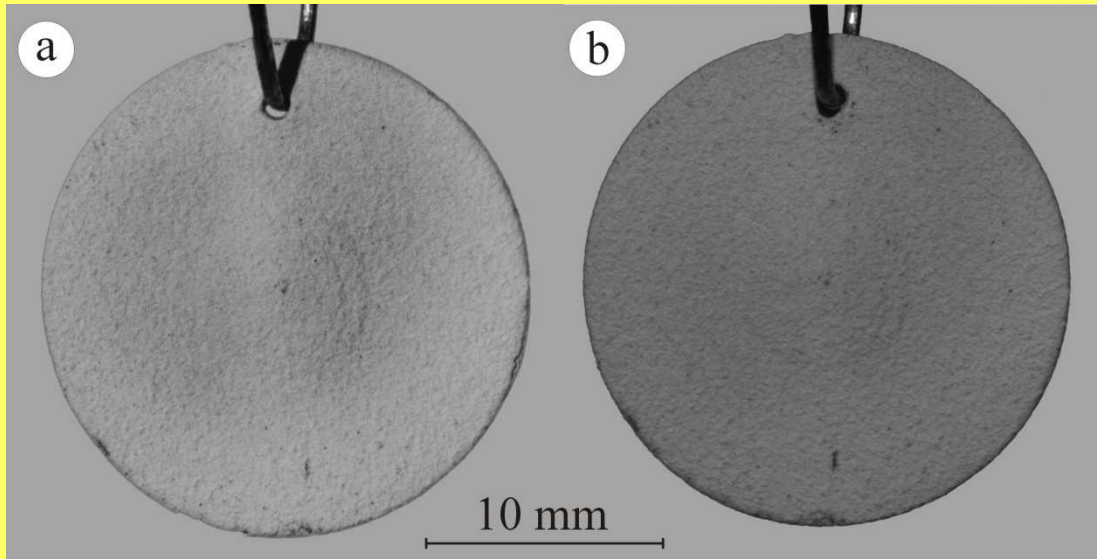
inner layer
of the coating

steel

Surface of TBC layer

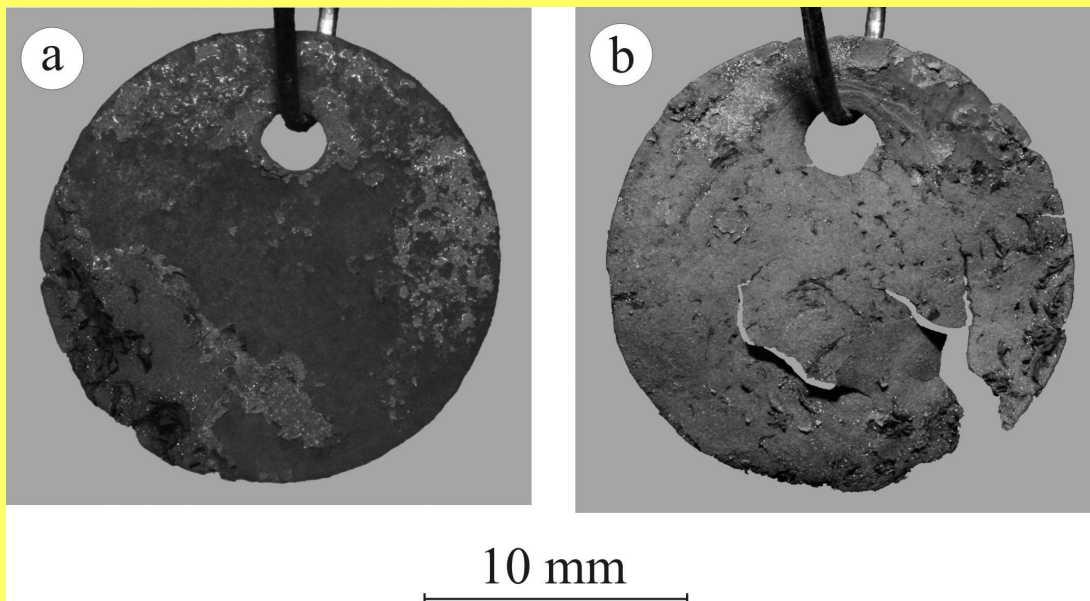


Photographs of surfaces of coated and uncoated valve steels after corrosion tests at 1173 K



a) before tests

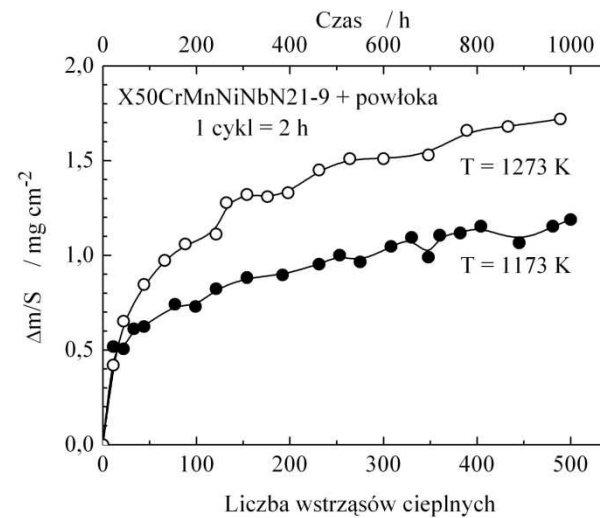
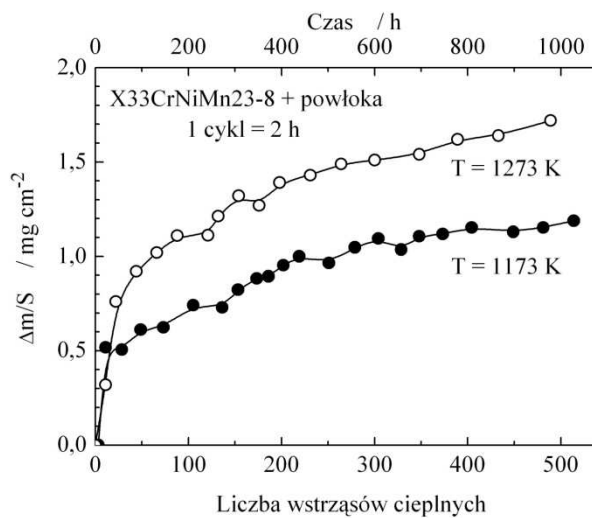
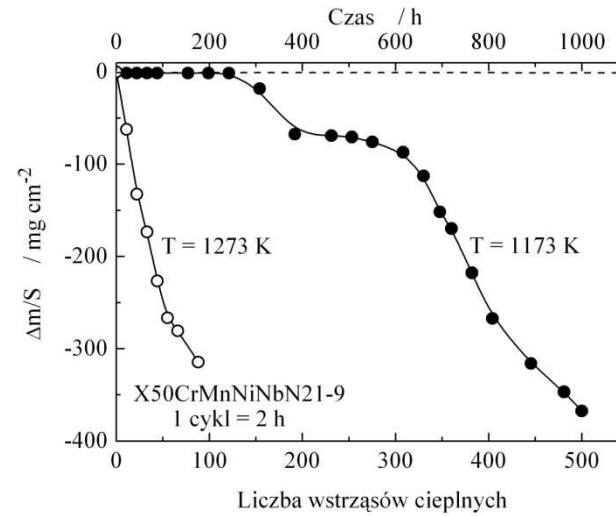
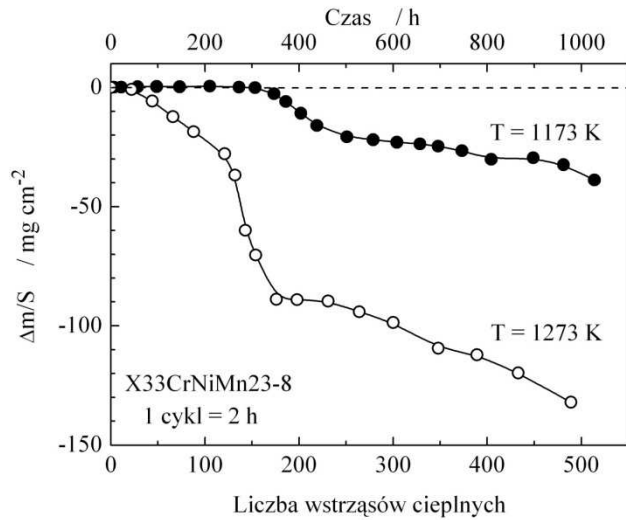
b) after 500 shocks



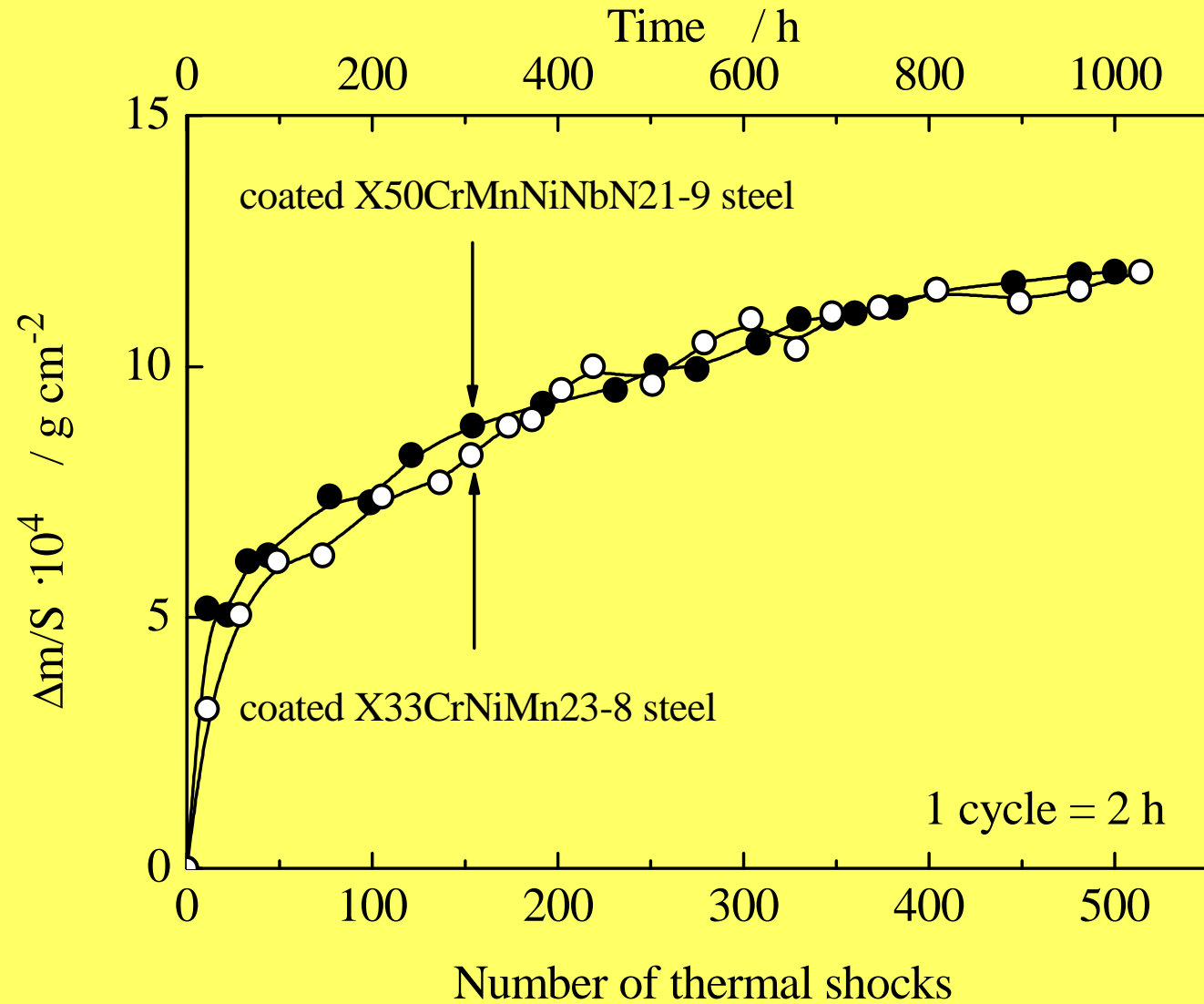
a) after 300 shocks

b) after 500 shocks

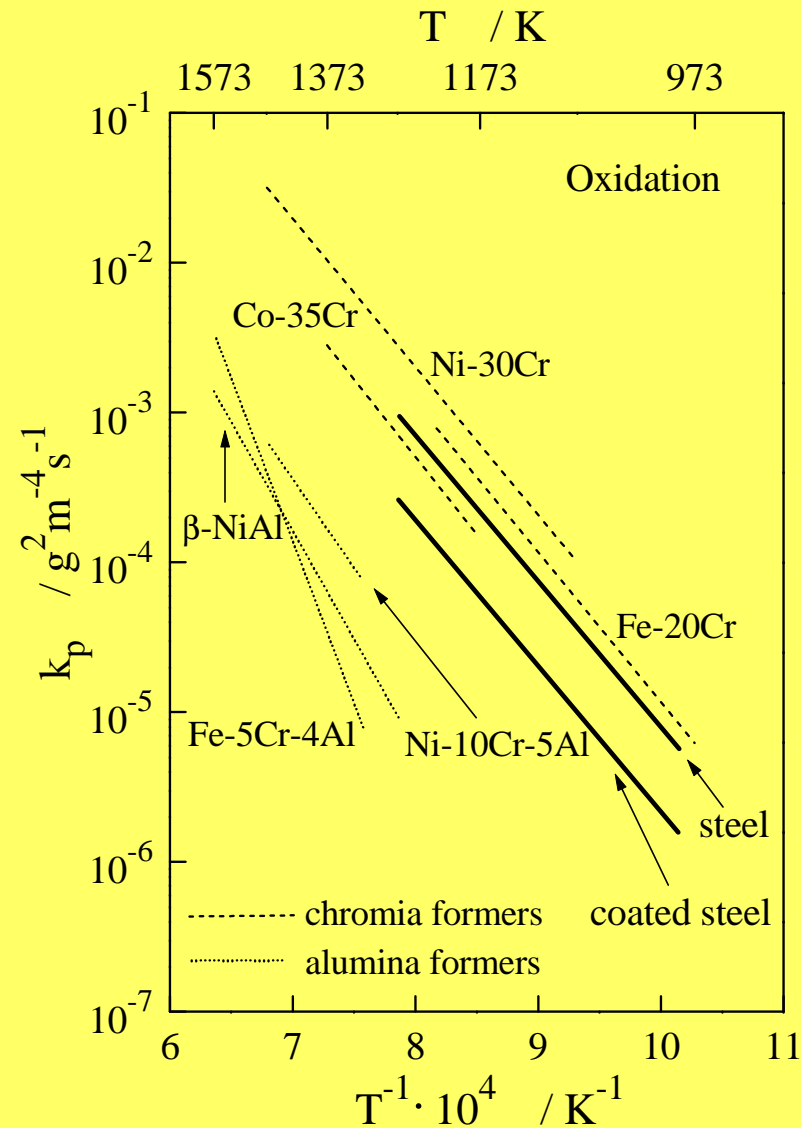
The results of corrosion tests of uncoated and coated valve steels



The results of corrosion tests of coated two different valve steels



Temperature dependence of the oxidation rate of steel coated with a protective coating



THE END